

This item is the archived peer-reviewed author-version of:

Expanding the squaramide library as mycobacterial ATP synthase inhibitors : innovative synthetic pathway and biological evaluation

Reference:

Chasák Jan, Oorts Lauren, Dak Milan, Šlachťová Veronika, Bazgier Václav, Berka Karel, De Vooght Linda, Smiejkowska Natalia, Van Calster Kevin, Van Moll Laurence,- Expanding the squaramide library as mycobacterial ATP synthase inhibitors : innovative synthetic pathway and biological evaluation
Bioorganic and medicinal chemistry - ISSN 1464-3391 - 95(2023), 117504
Full text (Publisher's DOI): <https://doi.org/10.1016/J.BMC.2023.117504>
To cite this reference: <https://hdl.handle.net/10067/2000120151162165141>

Expanding the squaramide library as mycobacterial ATP synthase inhibitors: innovative synthetic pathway and biological evaluation

Jan Chasák^{a,1}, Lauren Oorts^{b,1}, Milan Dak^a, Veronika Šlachťová^a, Václav Bazgier^c, Karel Berka^c, Linda De Vooght^b, Natalia Smiejkowska^b, Kevin Van Calster^b, Laurence Van Moll^b, Davie Cappoen^{b,+}, Paul Cos^b, Lucie Brulíková^{a,*}

^a*Department of Organic Chemistry, Faculty of Science, Palacký University, 17. listopadu 12, 77146, Olomouc, Czech Republic*

^b*Laboratory of Microbiology, Parasitology and Hygiene (LMPH), S7, Faculty of Pharmaceutical, Biomedical and Veterinary Sciences, University of Antwerp, Wilrijk, Belgium*

^c*Department of Physical Chemistry, Faculty of Science, Palacký University, 17. listopadu 12, 771 46, Olomouc, Czech Republic*

*Email: lucie.brulikova@upol.cz

¹These authors contributed equally.

⁺*Former affiliation and address during this project. New affiliation: Department of Food, Medicines and Consumer Safety, Scientific Institute of Public Health, Juliette Wytsmanstraat 14, Brussels, Belgium*

Abstract

Mycobacterial ATP synthase is a validated therapeutic target for combating drug-resistant tuberculosis. Inhibition of this enzyme has been featured as an efficient strategy for the development of new antimycobacterial agents against drug-resistant pathogens. In this study, we synthesised and explored two distinct series of squaric acid analogues designed to inhibit mycobacterial ATP synthase. Among the extensive array of compounds investigated, members of the phenyl-substituted sub-library emerged as primary hits. To gain deeper insights into their mechanisms of action, we conducted advanced biological studies, focusing on the compounds displaying a direct binding of a nitrogen heteroatom to the phenyl ring, resulting in the highest potency. Our investigations into spontaneous mutants led to the validation of a single point mutation within the *atpB* gene (Rv1304), responsible for encoding the ATP synthase subunit *a*. This genetic alteration sheds light on the molecular basis of resistance to squaramides. Furthermore, we explored the possibility of synergy between squaramides and the reference drug clofazimine using a checkerboard assay, highlighting the promising avenue for enhancing the effectiveness of existing treatments through combined

therapeutic approaches. This study contributes to the expansion of investigating squaramides as promising drug candidates in the ongoing battle against drug-resistant tuberculosis.

Keywords

Squaramides, tuberculosis, *Mycobacterium tuberculosis*, ATP synthase, antimycobacterial agents, MDR-TB.

1. Introduction

Mycobacterial adenosine triphosphate (*Mtb* ATP) synthase is a key enzyme in the energy metabolism of mycobacteria that has been found essential for the survival of bacteria under both replicating and non-replicating states [1,2]. Importantly, *Mtb* ATP synthase has been validated as a clinical target in treating drug-resistant tuberculosis [3–6]. Due to the significant structural differences between bacterial and mammalian ATP synthases, inhibition of *Mtb* ATP synthase is considered a relatively safe approach in treating multidrug-resistant (MDR) and extensively drug-resistant (XDR) *Mtb* infections. The discovery of the first ATP synthase inhibitor, bedaquiline **I** (Fig. 1), as a new class of antimycobacterial drug with a novel mode of action, has triggered the broad interest of medicinal chemists [1]. Bedaquiline **I**, developed by Janssen Pharmaceuticals, was found to target subunit *c* of *Mtb* ATP synthase [7]. Despite its significant efficiency against MDR *Mtb*, bedaquiline **I** has several drawbacks, such as a long half-life, high lipophilicity, low solubility, suffers from off-target effects and is susceptible to resistance mutations. Therefore, several research groups have focused on developing bedaquiline (BDQ) analogues with better safety profiles [5,8–13]. As an example, Blaser *et al.* (2019) synthesised analogues **II** and **III** (Fig. 1) with reduced cardiovascular toxicity [13]. Later, new scaffolds like thiazolidinediones, dihydropyrazolopyrazinones, diaminopyrimidines, diaminoquinazolines, chloroquinolines or squaramides appeared [1]. For example, a thiazolidinone derivative **IV** (Fig. 1) showed excellent anti-TB activity (*Mtb* H37Rv, MIC₉₀ = 0.5 µg/ml) with low cytotoxicity in human HepG2 cells [14]. Further, screening of chemically diverse compounds using *Mycobacterium smegmatis* (*Msm*) ATP synthase enzyme pointed out the 6,7-dihydropyrazolo[1,5-a]pyrazin-4-ones **V** (Fig. 1) as an attractive scaffold [15]. Interestingly, compound **V** does not inhibit any CYP450 enzymes and could be a starting point for further research in anti-TB drug discovery [15]. The most exciting compounds related to this study are squaramides, especially compound **VI** (Fig. 1), exhibiting nanomolar potencies in an ATP synthesis inhibition assay [16]. Studies on a membrane-based biochemical assay measuring ATP synthesis through oxidative phosphorylation suggested *Mtb* ATP synthase as a molecular target. Subsequently, Li *et al.* (2020) diversified the library of squaramides with diamino-substituted compounds (e.g. **VII**, Fig. 1) [17]. It is worth of notice that squaramides represent a unique feature that has received considerable attention from medicinal chemists [18].

Moreover, squaramides have found particular use as bioisosteric replacements of several heteroatomic functional groups like ureas, thioureas, guanidines, or cyanoguanidines, for instance [19].

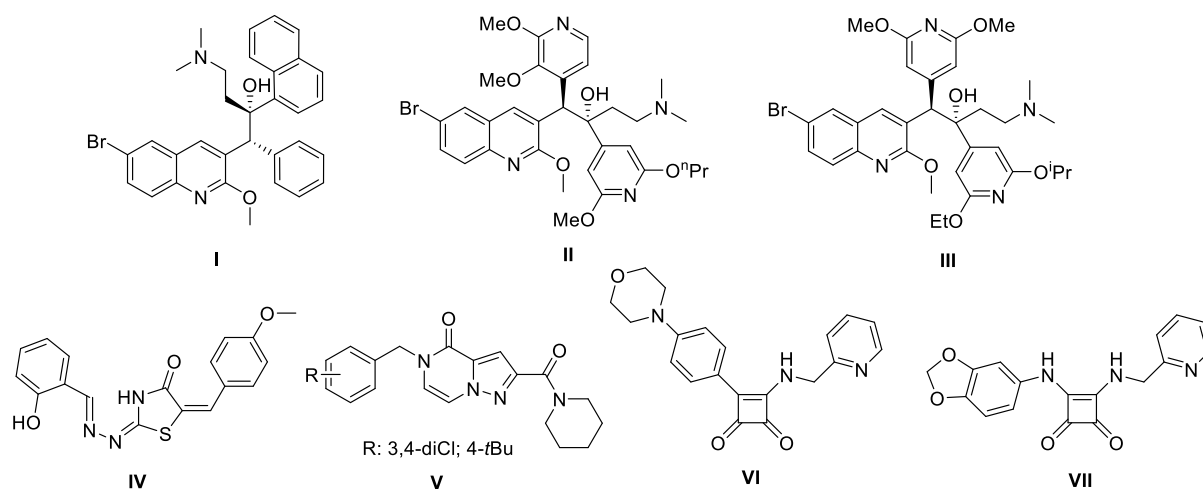


Figure 1: Structures of selected known *Mtb* ATP synthase inhibitors.

The structure–activity relationship (SAR) on squaramides performed by Tantry *et al.* (2017) [16] suggested that 2-pyridyl methyl substitution on the right-hand side (RHS) of the scaffold **VI** (Fig. 2) is crucial for reaching the desired potency. On the other hand, the left-hand side (LHS) of molecule **VI** is less explored. Tantry *et al.* studied only three different modifications on the LHS, where a morpholinophenyl moiety (compound **VI**, Fig. 2) was found to be the best. For this reason, we decided to explore further possibilities on the LHS and broaden the SAR study of squaramides. The first effort aimed to modify the aromatic moiety (Fig. 2, compounds **1**). Further, we focused on derivatives with an additional NH group to increase the hydrogen-bond interaction between the compound and ATP synthase (Fig. 2, compounds **2**).

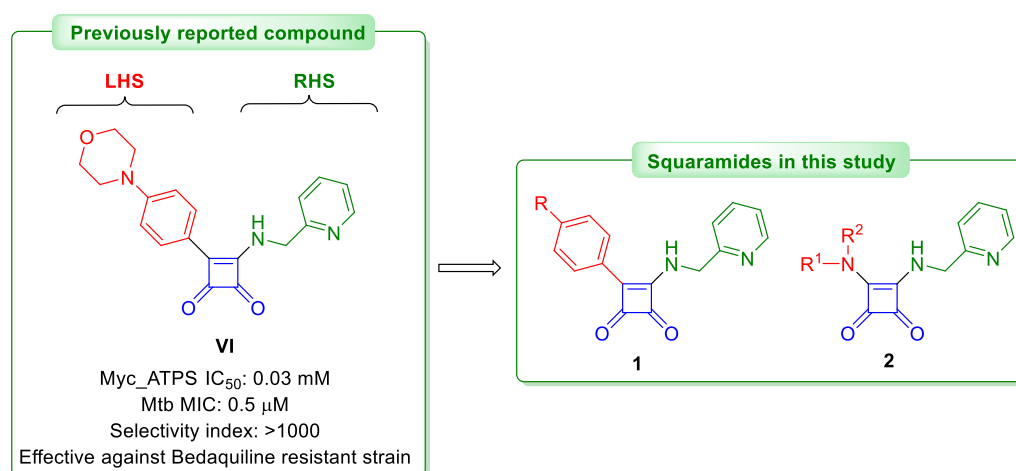


Figure 2: Design of new squaramides **1** and **2**.

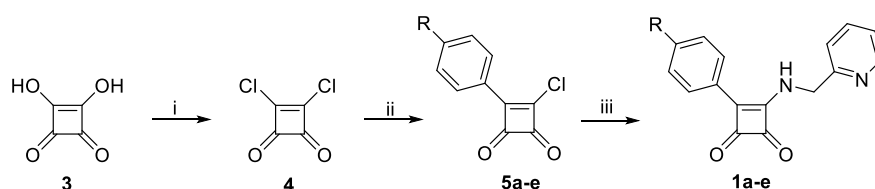
In this study, 30 squaramide analogues were designed, synthesised, and evaluated. Biological properties were assessed, and a subset of compounds was selected for further investigation based on their antimycobacterial activity. The biological validation consisted of assessing intracellular activity, validating the mode of action, and evaluating interaction with a reference compound, clofazimine (CFZ). Of particular interest is the checkerboard data, as treatment for tuberculosis typically requires combination therapy [20].

2. Results and discussion

2.1. Chemistry

2.1.1. Synthesis of target compounds **1a-e**

Our first synthetic effort leading to the target compounds **1** proceeded from the work published by Tantry et al. in 2017 [16] (Scheme 1). Based on their experiences, we used commercially available squaric acid **3** and converted it to the corresponding dichloro derivative **4**. Subsequently, crude dichloride **4** was subjected to arylation with various aromatic compounds in the presence of 0.25 equiv. AlCl₃ as Lewis acid giving precursors **5** (Scheme 1). Since the yields of this reaction were very low (1-23%), dichloride **4** was purified before use in the next step and was obtained in the 79% yield. Further, we increased the amount of AlCl₃ to 2 equiv. Finally, crude intermediates **5** were directly reacted with 2-(aminomethyl)pyridine in the presence of the base TEA, giving products **1a-e** in moderate to good yields (7-73% yield over two steps).

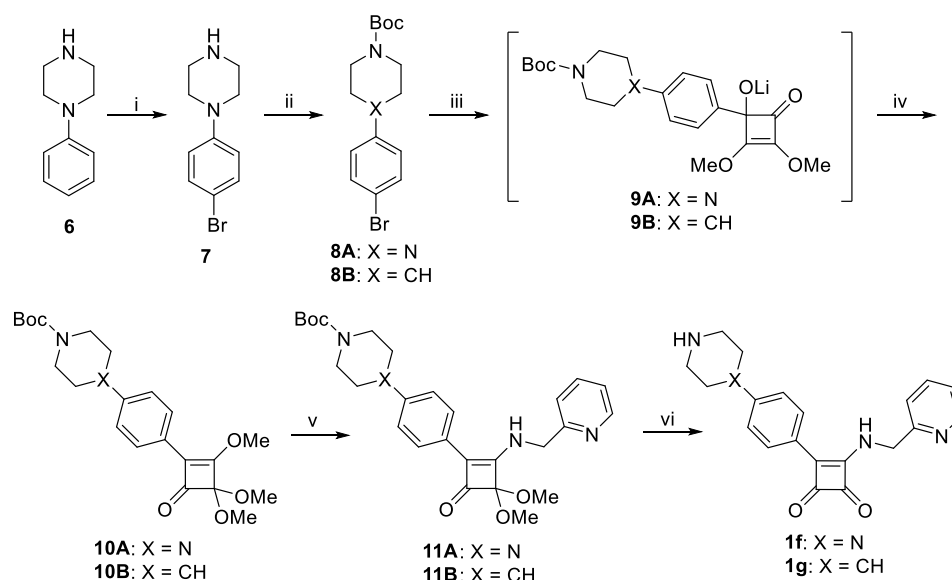


Scheme 1: Synthesis of target compounds **1a-e**. Reagents and conditions: (i) SOCl₂, DMF, 80 °C, 1 h, 79%; (ii) aryl compound, AlCl₃, DCM dry, 0 °C - rt, 2 h; (iii) 2-(aminomethyl)pyridine, 1,4-dioxane, TEA, 0 °C, 30 min, yields of 7-73%.

2.1.2. Synthesis of target compounds **1f-g**

Since the previous method failed during our efforts to introduce a 1-phenylpiperazine or 4-phenylpiperidine moiety into the final structure **1**, we were forced to modify this synthetic route (Scheme 2). Firstly, we had to prepare precursor **8A** through a reaction of 1-phenylpiperazine **6** with conc. HBr with subsequent protection of the NH group. Besides, we used commercially available precursor **8B**. Subsequently, 3,4-dimethoxycyclobut-3-ene-1,2-dione was treated with the *in situ* prepared lithium salt of **8** leading to intermediates **9**. The

addition of trifluoroacetic anhydride to the reaction solution with subsequent reaction termination with MeOH yielded monoketals **10**. Then, intermediates **10** were reacted with 2-(aminomethyl)pyridine giving derivatives **11**. Finally, the ketal and Boc protecting groups were removed using 10% HCl solution to afford the target compound **1f** in a 73% yield. TFA in DCM had to be added to remove protecting groups in the case of compound **1g** thoroughly.

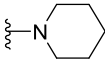
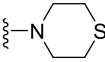
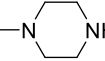
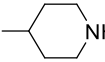
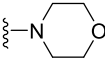


Scheme 2: Synthesis of target compounds **1f-g**. Reagents and conditions: (i) conc. HBr, DMSO, 60 °C, 1 h, 88%; (ii) (Boc)₂O, TEA, THF, 60 °C, 3 h, 86%; (iii) 3,4-dimethoxycyclobut-3-ene-1,2-dione, 1.7M *t*-BuLi, dry THF, -78 °C, 1-1.5 h; (iv) TFAA, MeOH, -78 °C - rt, 20 min, 51% for **10A** and 24% for **10B**; (v) 2-(aminomethyl)pyridine, MeCN, rt, 16 h, 95% for **11A** and 74% for **11B**; (vi) for **1f**: 10% HCl, DCM, rt, 15 min, 73%; for **1g**: 10% HCl, rt, 15 min; then TFA, DCM, rt, 2 h, 28%.

All compounds synthesised according to the Schemes 1 and 2 are briefly summarised in the Table 1. It is evident from this overview that some of the final derivatives were obtained in relatively low yields, what is mainly caused by the Friedel-Crafts type reaction step during the synthesis described in Scheme 1.

Table 1: Overview of the target compounds **1**.

Compds.	R	Yields (%)
1a		64
1b		53

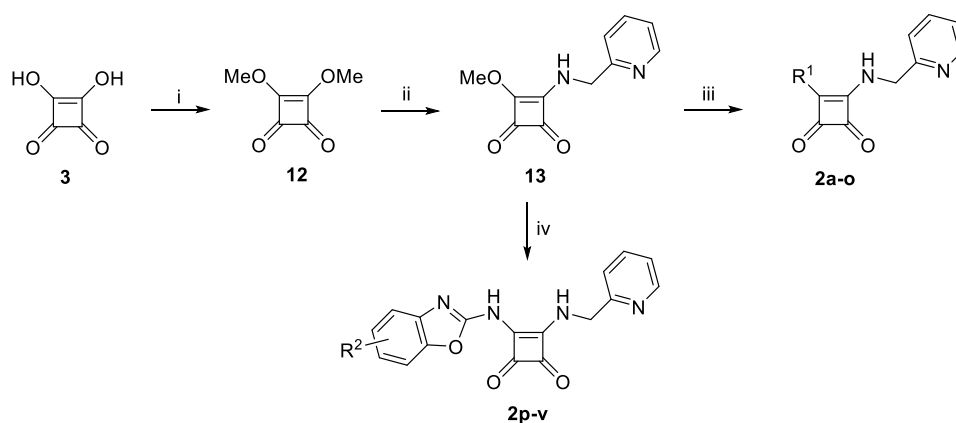
1c		73
1d		14
1e		7
1f		73
1g		28
1h*		7

*Compound published by Tantry et al. was synthesized according to published protocol [16].

2.1.3. Synthesis of target compounds **2a-v**

Further, we focused on synthesising derivatives **2** with an additional NH group to increase the hydrogen-bond interaction between the compound and ATP synthase. The performed molecular docking revealed relatively high binding constants for these derivatives, especially in the case of benzoxazole compounds **2p-v**. We also implemented a rather controversial nitro group to our structures selected mainly from the synthetic point of view to observe the relationship between structure and reactivity. On the other hand, although the nitro group is often considered a toxic moiety leading to mutagenicity and genotoxicity, many FDA-approved drugs contain nitro groups (eg. Pretomanid or Delamanid).

Synthesis of target compounds **2** is depicted in Scheme 3. Firstly, the dimethoxy derivative **12** from commercially available squaric acid was prepared. For this step, several solvents like MeOH, DMF or MeCN were tested. However, the best conversion proceeded in the presence of MeCN. Intermediate **12** was further reacted with 2-(aminomethyl)pyridine to give precursor **13**. Target compounds **2a-o** (Scheme 3) were synthesized by the reaction of **12** with various aliphatic, alicyclic or aromatic amines at room temperature or at 50 °C in moderate to high yield (33-87%, Table 2). On the other hand, the reaction of **12** with various 2-aminobenzoxazoles (prepared according to the described protocol [21]) required a higher reaction temperature (50 °C) and the presence of the base. Final compounds **2p-v** were obtained in low to moderate yield (8-50%, Table 3). Lower yields of some derivatives were caused by poor solubility and thus complicated purification.



Scheme 3: Synthesis of target compounds **2**. Reagents and conditions: (i) trimethylorthoformate, dry MeOH, 65 °C, 24 h, 89%; (ii) 2-(aminomethyl)pyridine, MeCN, rt, 40 min, 80%; (iii) amines, MeCN, rt or 50 °C (for derivative **2c**, **2g** and **2j**), 16 h, yields of 33-87%; (iv) 2-aminobenzoxazoles, DBU, MeCN, 50 °C, 16 h, yields of 8-50%.

Table 2: Overview of the target compounds **2a-o**.

Compds.	R ¹	Yields (%)
2a		69
2b		64
2c		20
2d		33
2e		69
2f		77
2g		48
2h		85

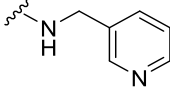
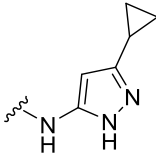
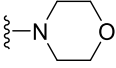
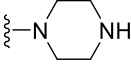
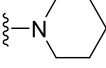
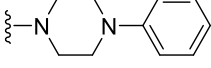
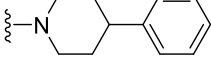
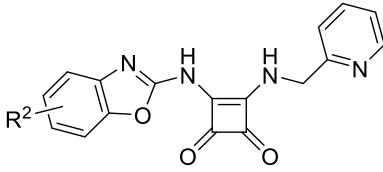
2i		65
2j		48
2k		33
2l		68
2m		72
2n		84
2o		71

Table 3: Overview of the target compounds **2p-v**.

		
Compds.	R ²	Yields (%)
2p	H	50
2q	5-Cl	47
2r	6-Cl	36
2s	5-CH ₃	21
2t	6-CH ₃	8
2u	5-NO ₂	33
2v	6-NO ₂	32

2.2. In vitro biological evaluation

2.2.1. Antimycobacterial activity

The minimum inhibitory concentration (MIC) of the test compounds (**1a-2v**) was assessed using the broth microdilution method. MIC was defined as the lowest concentration of the

antimicrobial agent that inhibits 90% of the mycobacterial growth. Data analysis revealed that the majority of compounds show no activity (>64 μM), some indicate weak activity (>10 μM) and four compounds (**1a**, **1d**, **1e** and **1h**) showed activity in the single digit micromolar range, indicating a powerful inhibitory effect on mycobacterial growth (Table 4). Compound **1e** showed comparable antimycobacterial activity to the previously reported compound [16], **1h**.

In addition to determining the potency of the active compounds, the minimal bactericidal concentration (MBC) was determined through a spot assay and full plating (Table 4). MBC, defined as the lowest concentration required to kill 99% of the bacterial population. For compounds **1a**, **1d**, **1e** and **1h** an MBC was found within the range of their predetermined MIC.

Furthermore, we evaluated cytotoxicity alongside the antimicrobial activity of all synthesised compounds. The results revealed no detectable cytotoxic effects associated with the most potent compounds. Based on these results, compounds **1a**, **1d**, and **1e** were selected for further validation. Compound **1h** was consistently included in the performed assays for comparison and BDQ served as reference drug throughout the experiments.

Table 4: Antimycobacterial activity, cytotoxicity, and partition coefficient **1a-2v**.

Compds.	logP ^a	H37Ra-Lux		RAW 264.7	
		MIC (μM) ^b	MBC (μM) ^c	CC ₅₀ (μM) ^d	SI ^e
1a	2.18	6.59 (\pm 2.17)	8 – 10	>64	>56.14
1b	2.48	14.93 (\pm 4.18)	>100	>64	>16.80
1c	4.45	>64	ND	>64	-
1d	3.29	2.56 (\pm 0.90)	1.20 – 2.00	>64	>177.78
1e	2.80	0.90 (\pm 0.28)	1.20 – 2.00	>64	>182.85
1f	1.91	19.88 (\pm 4.96)	64	>64	>3.21
1g	2.44	>64	ND	>64	-
1h	ND	0.77 (\pm 0.16)	0.40 – 1.20	>64	>492.31
2a	0.82	>64	ND	>64	-
2b	2.16	>64	ND	>64	-
2c	0.85	>64	ND	>64	-
2d	0.17	>64	ND	>64	-

2e	1.74	>64	ND	>64	-
2f	2.63	>64	ND	>64	-
2g	1.58	15.14 (\pm 6.60)	ND	>64	>6.01
2h	1.67	>64	ND	>64	-
2i	0.53	>64	ND	>64	-
2j	0.89	>64	ND	>64	-
2k	0.11	>64	ND	>64	-
2l	-0.21	>64	ND	>64	-
2m	1.18	>64	ND	>64	-
2n	2.06	>64	ND	26.25 (\pm 3.12)	<0.41
2o	2.60	>64	ND	7.47 (\pm 0.44)	<0.12
2p	1.61	>64	ND	>64	-
2q	2.22	>64	ND	>64	-
2r	2.22	>64	ND	>64	-
2s	2.13	>64	ND	>64	-
2t	2.13	>64	ND	>64	-
2u	1.55	>64	ND	>64	-
2v	1.55	>64	ND	>64	-
BDQ	ND	0.05 (\pm 0.02)	0.03 – 0.10	ND	-
Tamoxifen	ND	ND	ND	5.03 (\pm 0.21)	-

^a Log n-octanol/water partition coefficient determined by Chemaxon.

^b Lowest concentration that inhibits 90% growth compared to growth control, calculated using GraphPad Prism 9, nonlinear regression (variable slope).

^c Lowest concentration that reduces >99% of bacterial viability.

^d Cytotoxic concentration (CC), the concentration at which a 50% reduction in cellular viability was observed.

^e Selectivity index (SI): CC_{50} / IC_{50} (IC_{50} not shown).

The antimycobacterial activity of the tested compounds revealed that the phenyl moiety directly bound to the squaric cycle is essential for reaching the desired potency (Fig. 3,

compounds **1**). On the other hand, the introduction of an amine bond (in the case of compounds **2**) resulted in a marked loss of activity. In addition, the presence of a nitrogen heteroatom directly bound to the phenyl ring proved to be relevant for increasing *in vitro* activity (compounds **1d**, **1e**, **1f**, **1h**). In contrast, a remarkable negative effect was obtained upon replacement of the nitrogen heteroatom with a CH group (compounds **1c** and **1g**).

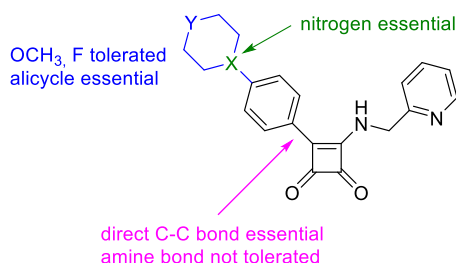


Figure 3: Summary of the SAR study.

2.2.2. Mode of action: Squaramides target the ATP synthase F₀ complex subunit a

This particular set of compounds is known to target the ATP synthase. However, to determine the exact mechanism of inhibition within this complex enzyme, we endeavoured to create spontaneous mutants. To generate resistant strains, H37Ra inoculum was exposed to a 10-fold and 16-fold MIC concentration of selected compounds on 7H11 agar plates. While compound **1e** proved to be unstable and lost activity due to the pre-heated agar, **1a** and **1d** successfully produced resistant colonies. The resistance frequency (m) was determined *via* the equation $m = N_m/N_t$, where N_m represents the number of mutants ($N_m = 26$) and N_t the total number of cells ($N_t = 6.6 \times 10^7$), resulting in a frequency (m) of approximately 4×10^{-7} . In total, 10 colonies were isolated for further validation.

A panel of 9 genes, listed in the experimental section were amplified from the isolated gDNA of the 10 resistant strains and a wild type as reference. Analysis revealed an unambiguous result. For each resistant strain, the DNA sequence encoding residue 179 from the *atpB* gene spontaneously changed from AAG to AAT. This substitution in ATP synthase subunit *a* resulted in the original lysine being replaced with an asparagine. MIC values of these newly generated mutants were re-evaluated, resulting in a value of $>300 \mu\text{M}$ which was limited by the maximum permitted DMSO concentration.

2.2.3. Spontaneous mutants remain prone to BDQ

Although BDQ inhibits ATP synthase by targeting the *c*-subunit, complete binding may require alterations in the structural conformation of subunit *a* [22]. To investigate the influence of K179N substitution on the BDQ sensitivity, the MIC was investigated for two resistant strains.

The sensitivity was evaluated using Resazurin microtiter assay (REMA) in a 3-fold serial dilution of BDQ starting from 10 μM , in triplicate. Fig. 4 illustrates no alteration in the dose-response curve and the calculated MICs remained within normal range. The MIC values recorded were 0.11 μM , 0.12 μM , and 0.10 μM for atpB.K179N_01, atpB.K179N_02, and WT, respectively. These results indicate that the point mutation caused by squaramides neither interfere with the binding site, nor with the mode of inhibition of BDQ.

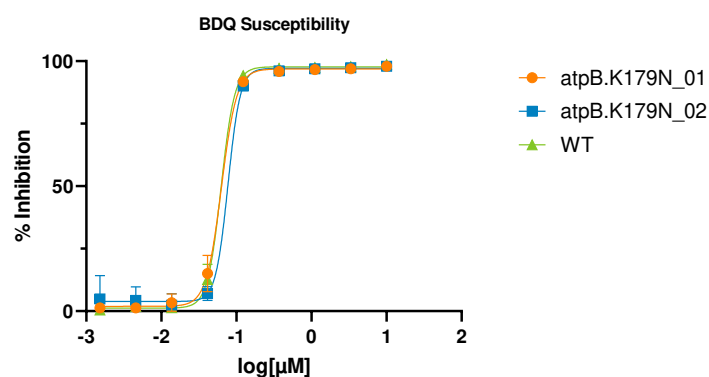


Figure 4: Bedaquiline (BDQ) sensitivity against squaramide mutants. Dose response curve of 3 H37Ra strains (atpB.K179N_01, atpB.K179N_02 and WT) treated with BDQ ranging from 0.002-10 μM in triplicate. Results were processed using GraphPad Prism 9 nonlinear regression (variable slope – four parameters).

2.2.4. Time-Kill assay and Immunofluorescence

The **Time-Kill Macrophage Infection assay** was performed to investigate the intracellular bactericidal activity of the selected test compounds. The assay was conducted using a murine cell line, RAW 264.7, infected with H37Ra-Lux at a multiplicity of infection (MOI) of 10. According to their individual MIC values, a 2-fold serial dilution of each test compound was set up in triplicate to evaluate their intracellular activity. Fig. 5A indicates the time-kill kinetics at three different time points for a DMSO control (growth control and the four selected compounds at 0.5x, 1x and 2x their individual MIC values. 24h post-infection, a deviation from the growth control was observed for compound **1a**, this deviation was seen in multiple independent repeats without a reasonable explanation. Notifying the error bars, it can be assumed that there was no effect after 24h of compound exposure. Altogether, **1a** appears to be the least potent intracellular inhibitor. Looking at the kill kinetics for the MIC graph, all compounds show nearly the same activity after 72h. However, after 24h, compound **1d** appears to be the most effective, a similar trend but less pronounced can be observed in the 0.5xMIC graph. The graph showing response of 2xMIC values depicts a prompt and extreme response. Overall, this data indicates efficacious intracellular activity aligning with the

compounds' antimicrobial properties, highlighting a minor intracellular superiority exhibited by compound **1d**.

The intracellular activity of the prioritised compound **1d** was validated by **immunofluorescence**. Macrophages were infected with a red fluorescent reporter strain (*H37Ra.mScarlet*⁺) and subsequently exposed for 72h to 4 μ M **1d** or DMSO (DMSO concentration remained identical for both conditions). In Fig. 5B mycobacteria are visualised in DMSO-treated cells, suggesting successful infection. Despite the challenging quantification of infection due to clump formation, an 80-90% decrease in bacterial load could be observed in **1d** treated cells.

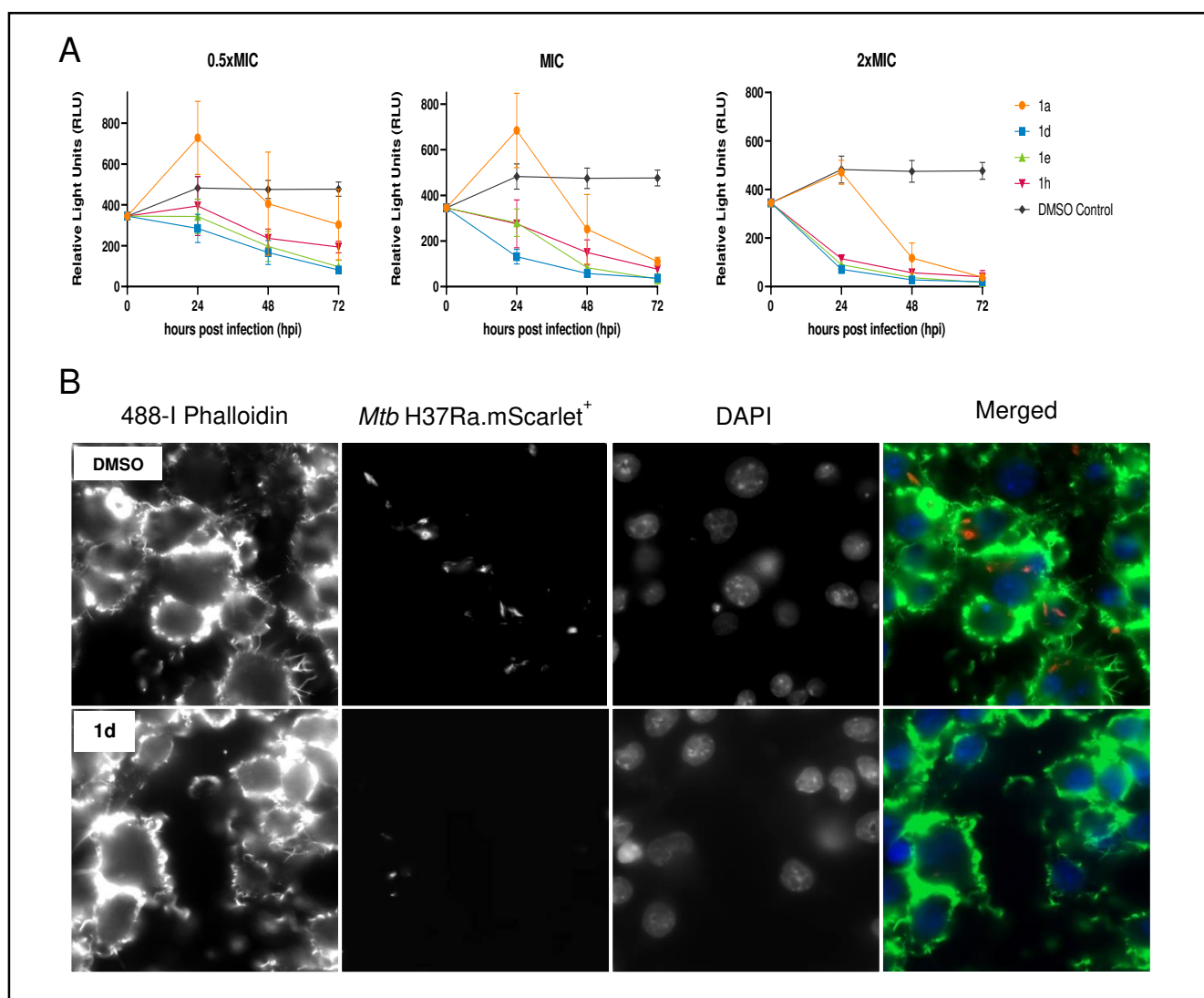


Figure 5: Antimycobacterial activity in murine macrophages (RAW 264.7). (A) time-kill kinetics of compounds **1a** (orange), **1d** (blue), **1e** (green), **1h** (pink) and a DMSO control (black) for different concentration with respect to the corresponding compounds. Activity was monitored at 3 time points post infection (24, 48 and 72h) and data is displayed as the mean \pm SD of Relative Light Units (RLU).

(B) Intracellular monitoring of H37Ra macrophage infection and the effect of squaramide treatment. RAW 264.7 macrophages were infected with H37Ra.mScarlet+ (Red) and treated with compound 1d for 72h. Actin filaments and cell nucleus were stained with 488-I Phalloidin (green) and DAPI (blue), respectively. The cells were visualized and captured using a ZEISS Axio Observer Z1 microscope at 63x magnification, images were processed using ZEN software.

2.2.5. Checkerboard assay uncovered synergy between squaramides and a reference drug

The interaction between the squaramides and reference drug, CFZ was evaluated in the checkerboard assay. CFZ is a second-line drug used in combination therapy for MDR-TB that disrupts the bacterial energy metabolism by interfering with the mycobacterial respiratory chain and potassium transport [23]. Given its mode of action, it was apparent to investigate the CFZ-squaramide interaction. The synergy was evaluated by calculating FICI's and establishing an Isobole based on IC₅₀. Fig. 6 displays a tendency towards synergy for each compound. However, it is noteworthy that this perspective is not highly rigorous, yet it provides an insightful understanding of the interplay between the two compounds. Furthermore, the observed IC₅₀ for CFZ in combination with **1e** is lower than the anticipated value, we acknowledge this slight discrepancy as normalization was conducted for the entire plate, and experiments were performed in triplicate. The assessment of interactions was accomplished by calculating the FIC index displayed in Table 5. An additive or unchanged effect was observed for **1a**, **1e** displays a FIC index at the border of a synergistic interaction and both **1d** and **1h** demonstrate a synergistic effect with FICI values of 0.29 (± 0.09) and 0.37 (± 0.03), respectively.

Table 5: Checkerboard interactions based on fractional inhibitory concentration index (FICI), between Clofazimine (CFZ) and squaramides **1a**, **1d**, **1e** and **1h**

Drug combination	FICI	Interaction
1a + CFZ	0.63 \pm 0.13	Indifference
1d + CFZ	0.29 \pm 0.09	Synergistic
1e + CFZ	0.48 \pm 0.05	Synergistic/Additive
1h + CFZ	0.37 \pm 0.03	Synergistic

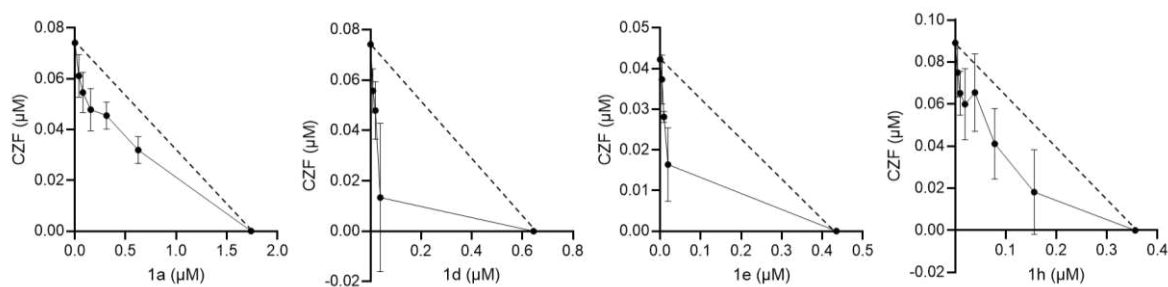


Figure 6: Isobologram-based characterization of squaramides (**1a**, **1d**, **1e**, **1h**) vs. Clofazimine (CFZ). To construct the isobologram, the IC_{50} values were determined in triplicate for various combinations. A point positioned below the dotted line is indicative of a synergistic effect, while a point lying on the dotted line suggests an additive effect and a point positioned above signifies an antagonistic effect.

2.3. *In silico* molecular docking

Squaramide structures were also docked into a model of ATP synthase. Since no experimental structure is available for *Mtb*, we have generated a homology model built using SwissModel server [26] over *Msm* structure PDBID:7NJP. Since both Mycobacteria share similar sequences with more than 75% identity, we have first docked squaramides using Autodock Vina [27] into structures from *Msm* in various states (PDBID:7NJK [state 1a], 7NJP [state 2], 7NJQ [state 3a], 7JGA [state 3 with BDQ]) [28,29]. We have identified, that squaramides bind specifically into the cavity in between rotating *c*-subunit and static *a*-subunit, with preference for state 2 (Fig. 7). ATP synthase complex states differ in the relative position between both subunits followed by the movement of individual amino acids – state 2 is specific in the rotation of subunit *a* (coded by *Msm atpB* gene) with E177 (*Mtb* eq. E175) residue inwards to interact with K181 residue (*Mtb* eq. K179), whereas in other states it interacts with *c*-subunit (coded by *atpE* gene). Squaramides (see Fig. 7) bound with RHS directly interacting with this residue. LHS containing nitrogen as a hydrogen bond acceptor is interacting with *Msm* N174 (*Mtb* eq N172; part of subunit *a*). Most contacts to *c*-subunit are then provided by nonpolar interactions - e.g., *Msm* I59 (*Mtb* eq. I55).

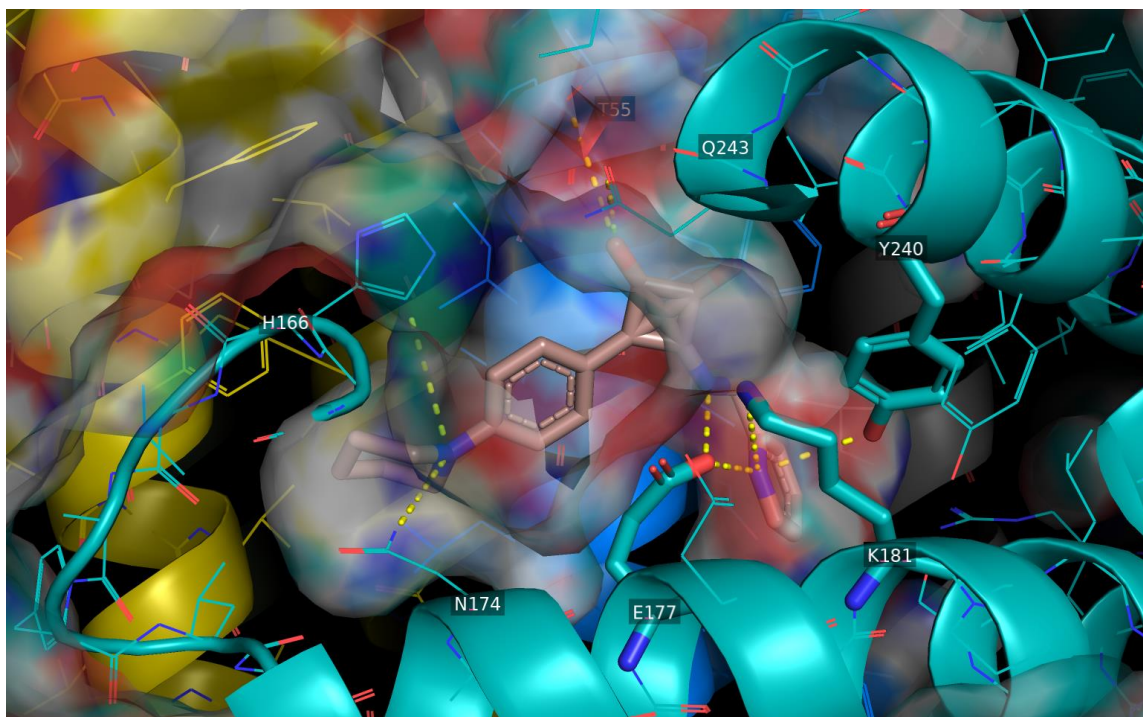


Figure 7: Binding pose for compound **1d** into *Msm* ATP synthase in state 2 – PDBID:7NJP. Subunit *a* is shown with cyan cartoon, *c*-subunit is shown in yellow and green colours in the background.

Squaramides are thus fitting to the interface between subunits *c* and *a* effectively blocking movement of the rotating *c*-subunit by the binding to *Msm* E177 residue on subunit *a*. This binding motif was retained also in the *Mtb* SwissModel model E175 based on structure 7NJP (see Fig. 8). However, the binding site of squaramides is different to the position of BDQ binding (see Fig. 9) – which can explain why they are efficient also against BDQ-resistant strains. Finally, according to the results of docking, squaramides bind less effectively to the *Mtb* structure, where K179 is mutated to N179 (subunit *a*).

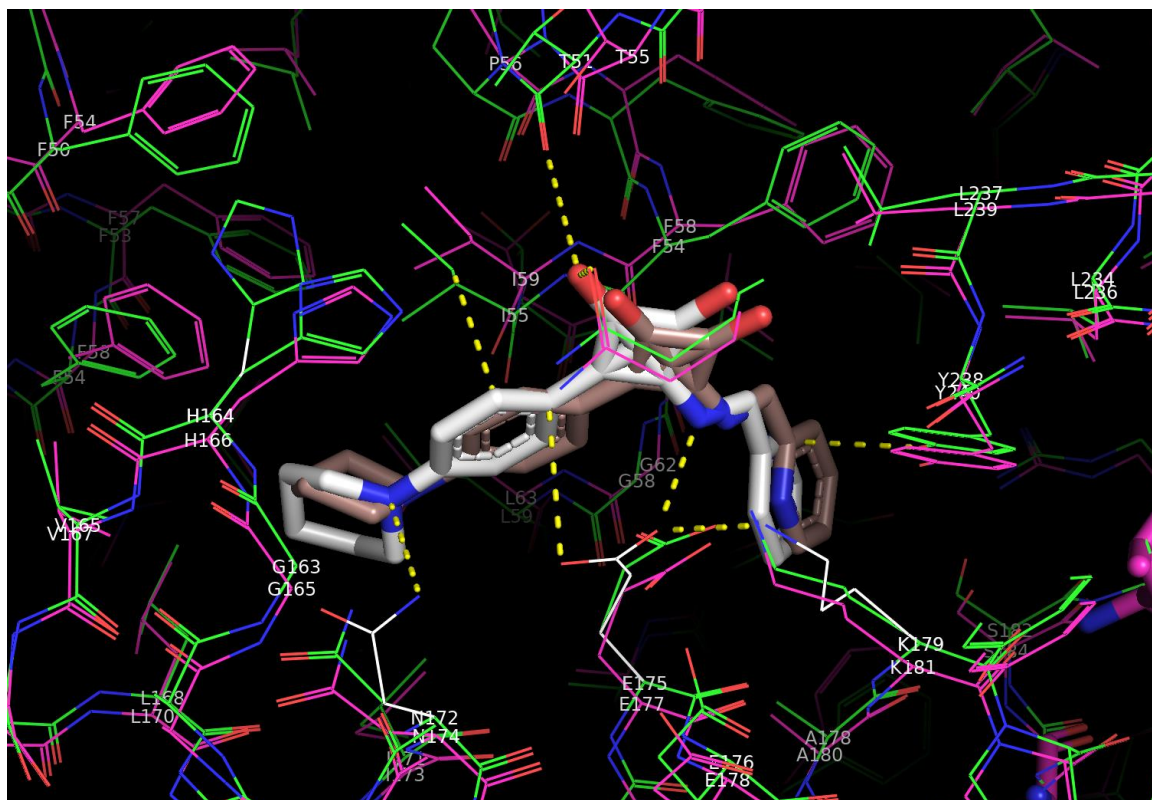


Figure 8: Comparison of binding poses of compound **1d** to *Mtb* ATP synthase model (white and green) and *Msm* ATP synthase in state 2 (brown and magenta, PDBID:7NJP). Both binding sites contain almost the same amino acid composition. White residues on *Mtb* structure show positions of flexible side chains used in docking (H164, N172, E175, K179).

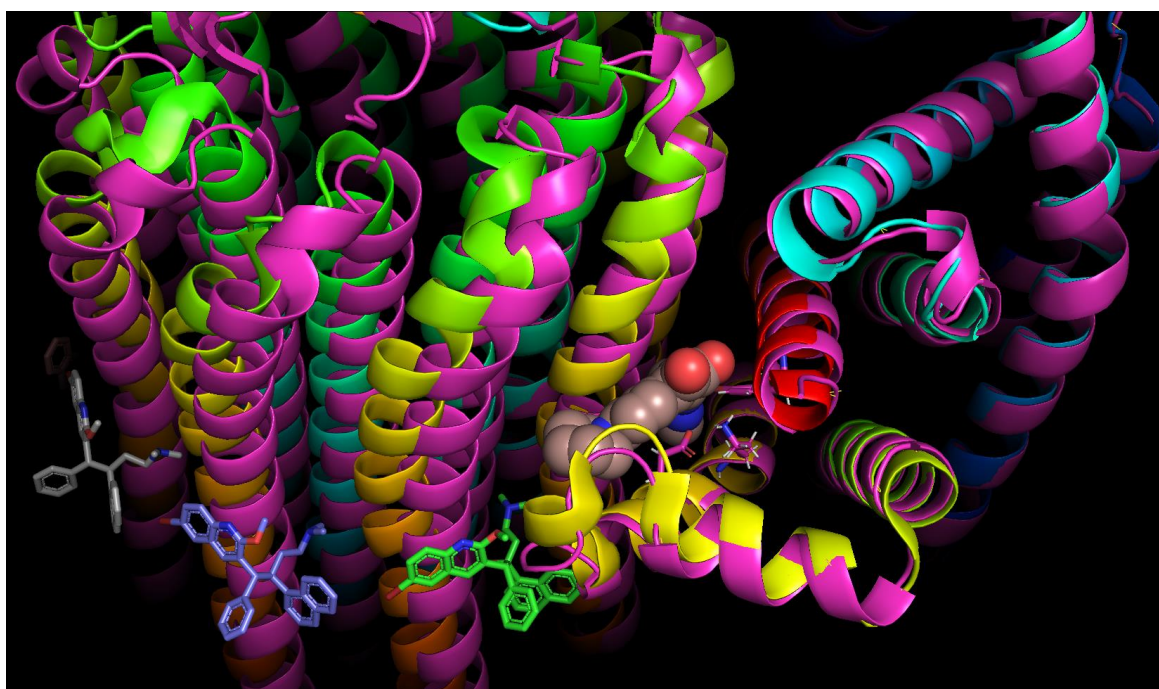


Figure 9: Comparison of binding of compound **1d** (brown spheres) and BDQ (sticks) to their respective structures – *Mtb* model of state 2 (magenta) and *Msm* ATP synthase in state 3 (multicolour cartoons, PDBID:7JGA). Note not only the different position of both compounds, when bulkier BDQ blocks the

rotation of the c subunit from the surface of the complex, but also the relative position shift of c-subunit between both structures aligned over a-subunit.

3. Conclusion

To conclude, we prepared 30 novel squaramides (designed based on *in silico* assays) targeting subunit a of mycobacterial ATP synthase. The synthetic part of the paper describes in the details a new methodology for C-C bond formation to bind an aromatic substituent to the central squaric acid skeleton. Biological testing results indicate that an aromatic substituent bearing a heteroatom capable of acceptor-hydrogen bonding is essential for the activity of the target compounds. From the insight into the active site of the target enzyme, it is evident that this hydrogen interaction with *Mtb* ATP synthase residue N172 is crucial for the "retention" of the molecule in the binding site. Interactions of the nitrogen heteroatoms of the 2-aminomethylpyridine substituent (with E175, K179 and Y238) also play an important role. The most active of the tested compounds showed submicromolar MICs. Using these derivatives, we were also able to experimentally verify the binding site of squaramide derivatives to mycobacterial ATP synthase by the creation of spontaneous mutants. Moreover, the uncovered synergy of squaramides and the reference drug, clofazimine, might provide new opportunities for combination therapies to combat antimicrobial resistance. Although promising, further research regarding safety assessment, *in vivo* validation and evaluation against clinical *Mtb* strains are needed.

4. Experimental section

4.1. Materials and Methods

Solvents and chemicals were purchased from Sigma-Aldrich (St. Louis, Missouri, USA) or Fluorochem (UK). Analytical thin-layer chromatography (TLC) was performed using aluminium plates precoated with silica gel 60 F254. All reactions were carried out at room temperature (21 °C) unless stated otherwise.

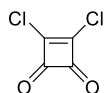
The LC-MS analyses were carried out on the UHPLC-MS system (Waters). This system consists of UHPLC chromatograph Acquity with photodiode array detector and single quadrupole mass spectrometer and uses a XSelect C18 column (2.1 x 50 mm) at 30 °C and flow rate of 600 µl/min. The mobile phase was (A) 10 mM ammonium acetate in HPLC grade water and (B) HPLC grade acetonitrile. A gradient was formed from 10% A to 80% B in 2.5 minutes; kept for 1.5 minutes. The column was re-equilibrated with a 10% solution of B for 1 minute. The ESI source operated at a discharge current of 5 µA, vaporizer temperature of 350 °C and capillary temperature of 200 °C.

NMR $^1\text{H}/^{13}\text{C}$ spectra were recorded on JEOL ECX-500SS (500 MHz) or JEOL ECA400II (400 MHz) spectrometer at magnetic field strengths of 11.75 T (with operating frequencies 500.16 MHz for ^1H and 125.77 MHz for ^{13}C) and 9.39 T (with operating frequencies 399.78 MHz for ^1H and 100.53 MHz for ^{13}C) at ambient temperature ($\sim 21\text{ }^\circ\text{C}$). Chemical shifts (δ) are reported in parts per million (ppm) and coupling constants (J) are reported in Hertz (Hz). NMR spectra are recorded at rt ($21\text{ }^\circ\text{C}$) and referenced to the residual signals of $\text{DMSO-}d_6$.

HRMS analysis was performed on LC chromatograph (Dionex UltiMate 3000, Thermo Fischer Scientific, MA, USA) with mass spectrometer Exactive Plus Orbitrap high-resolution (Thermo Fischer Scientific, MA, USA) operating in positive scan mode in the range of 1000–1500 m/z. Electrospray was used as a source of ionization. Samples were diluted to a final concentration of 0.1 mg/ml in a solution of water and acetonitrile (50:50, v/v). The samples were injected into the mass spectrometer following HPLC separation on a Phenomenex Gemini column (C18, 50 x 2 mm, 3 μm particle) using an isocratic mobile phase of 0.01 M MeCN/ammonium acetate (80/20) at a flow rate of 0.3 ml/min. For compounds containing chlorine or bromine atom only one isotope is stated (^{35}Cl and ^{79}Br).

4.2. Chemistry

4.2.1. 3,4-Dichlorocyclobut-3-ene-1,2-dione **4**



Squaric acid **3** (1 g; 8.77 mmol) was suspended in SOCl_2 (1.28 ml; 17.54 mmol), and DMF was added in a catalytic amount. The reaction mixture was stirred under reflux at $80\text{ }^\circ\text{C}$ for 1 h. After the reaction was complete, SOCl_2 was evaporated under reduced pressure and residue was crystallized from hot hexane. The product was obtained as a yellow solid. Yield: 1041.5 mg (79%). ^{13}C NMR (101 MHz, CDCl_3) δ 189.6, 188.2.

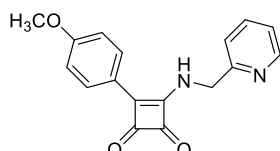
4.2.2. General procedure for the synthesis of **5a-e**

Compound **4** (500 mg, 3.31 mmol) was dissolved in dry DCM (10 ml). The solution was cooled to $0\text{ }^\circ\text{C}$, and AlCl_3 (883 mg, 6.62 mmol) and an appropriate aryl compound (3.31 mmol) were added. The reaction mixture was stirred at rt for 1.5 h. After that, the mixture was poured onto ice, and the product was extracted into DCM (3 x 20 ml). Combined organic layers were washed with brine (10 ml), water (10 ml) and dried over anhydrous MgSO_4 . The solvent was evaporated under reduced pressure, and obtained crude product was used in the next step without further purification.

4.2.3. General procedure for the synthesis of **1a-e**

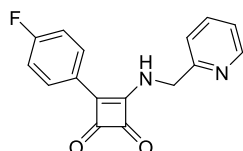
The crude product **5** was dissolved in 10 ml of 1,4-dioxane, and the solution was cooled to 0 °C. Next, TEA (1.0 eq.) and 2-(aminomethyl)pyridine (1.5 eq.) were added, and the reaction mixture was stirred at rt for 30 min. The solvent was evaporated under reduced pressure, and the residue was suspended in water (5 ml). The suspension was filtered, and the precipitated solid was washed with water. The final product was purified by column chromatography using Hex/EtOAc (grad.).

4.2.3.1. 3-(4-Methoxyphenyl)-4-((pyridin-2-ylmethyl)amino)cyclobut-3-ene-1,2-dione **1a**



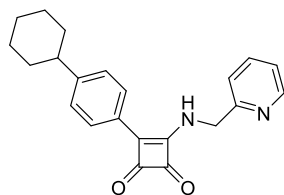
The product **1a** was obtained as a white solid. Yield: 624 mg (64%). ¹H NMR (400 MHz, DMSO-*d*₆) δ 9.50 (t, *J* = 6.1 Hz, 1H), 8.56 (ddd, *J* = 4.8, 1.7, 0.9 Hz, 1H), 8.05 – 8.02 (m, 2H), 7.81 (td, *J* = 7.7, 1.8 Hz, 1H), 7.45 (d, *J* = 7.8 Hz, 1H), 7.32 (ddd, *J* = 7.5, 4.9, 0.9 Hz, 1H), 7.14 – 7.09 (m, 2H), 5.02 (d, *J* = 6.2 Hz, 2H), 3.84 (s, 3H). ¹³C NMR (101 MHz, DMSO-*d*₆) δ 192.45, 188.9, 178., 162., 161.1, 157.2, 149., 137.0, 128.3, 122.7, 122.1, 121.6, 114.6, 55.4, 48.8. HRMS: *m/z*: calcd. for C₁₇H₁₅N₂O₃⁺: 295.1077 [M+H]⁺; found: 295.1079.

4.2.3.2. 3-(4-Fluorophenyl)-4-((pyridin-2-ylmethyl)amino)cyclobut-3-ene-1,2-dione **1b**



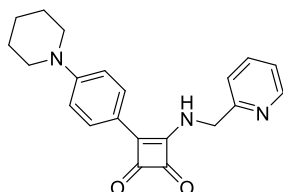
The product **1b** was obtained as a white solid. Yield: 496 mg (53%). ¹H NMR (400 MHz, DMSO-*d*₆) δ 9.68 (t, *J* = 6.1 Hz, 1H), 8.56 (ddd, *J* = 4.8, 1.6, 0.8 Hz, 1H), 8.14 – 8.08 (m, 2H), 7.82 (td, *J* = 7.7, 1.8 Hz, 1H), 7.46 (d, *J* = 7.8 Hz, 1H), 7.45 – 7.37 (m, 2H), 7.33 (ddd, *J* = 7.5, 4.9, 0.9, 1H), 5.02 (d, *J* = 6.2 Hz, 2H). ¹³C NMR (101 MHz, DMSO-*d*₆) δ 193.1, 188.7, 179.0, 163.0 (d, *J* = 250.2 Hz), 160.5, 157.0, 149., 137.1, 128.7 (d, *J* = 8.7 Hz), 126.0 (d, *J* = 2.9 Hz), 122.7, 121.7, 116.2 (d, *J* = 21.9 Hz), 48.9. HRMS: *m/z*: calcd. for C₁₆H₁₂FN₂O₂⁺: 283.0877 [M+H]⁺; found: 283.0871.

4.2.3.3. 3-(4-Cyclohexylphenyl)-4-((pyridin-2-ylmethyl)amino)cyclobut-3-ene-1,2-dione **1c**



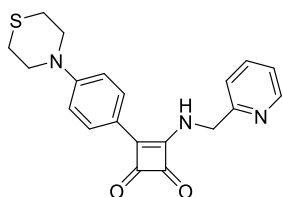
The product **1c** was obtained as a white solid. Yield: 838 mg (73%). ¹H NMR (400 MHz, DMSO-*d*₆) δ 9.56 (t, *J* = 6.1 Hz, 1H), 8.57 – 8.52 (m, 1H), 7.9 (d, *J* = 8.3 Hz, 2H), 7.81 (td, *J* = 7.7, 1.9 Hz, 1H), 7.44 (d, *J* = 7.9 Hz, 1H), 7.40 (d, *J* = 8.3 Hz, 2H), 7.32 (dd, *J* = 7.6, 4.8 Hz, 1H), 5.01 (d, *J* = 5.9 Hz, 2H), 2.62 – 2.52 (m, 1H), 1.83 – 1.66 (m, 5H), 1.49 – 1.19 (m, 5H). ¹³C NMR (101 MHz, DMSO-*d*₆) δ 193.1, 188.9, 179.1, 162.1, 157.1, 150.7, 149.3, 137.1, 127.3, 127.0, 126.4, 122.7, 121.6, 48.9, 43.9, 33.6, 26.2, 25.5. HRMS: *m/z*: calcd. for C₂₂H₂₃N₂O₂⁺: 347.1754 [M+H]⁺; found: 347.1753.

4.2.3.4. 3-(4-(Piperidin-1-yl)phenyl)-4-((pyridin-2-ylmethyl)amino)cyclobut-3-ene-1,2-dione **1d**



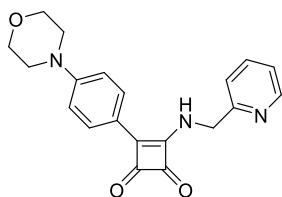
The product **1d** was obtained as a white solid. Yield: 161 mg (14%). ¹H NMR (400 MHz, DMSO-*d*₆) δ 9.32 (t, *J* = 6.2 Hz, 1H), 8.55 (ddd, *J* = 4.8, 1.6, 0.8 Hz, 1H), 7.92 (d, *J* = 9.0 Hz, 2H), 7.81 (td, *J* = 7.7, 1.8 Hz, 1H), 7.42 (d, *J* = 7.8 Hz, 1H), 7.31 (ddd, *J* = 7.5, 4.9, 0.8 Hz, 1H), 7.02 (d, *J* = 9.1 Hz, 2H), 5.00 (d, *J* = 6.2 Hz, 2H), 3.36 (br s, 4H), 1.59 (s, 6H). ¹³C NMR (101 MHz, DMSO-*d*₆) δ 191.5, 189.0, 177.8, 163.2, 157.5, 152.3, 149.2, 137.0, 128.2, 122.6, 121.5, 118.0, 113.9, 48.8, 47.8, 24.9, 23.9. HRMS: *m/z*: calcd. for C₂₁H₂₂N₃O₂⁺: 348.1707 [M+H]⁺; found: 348.1707.

4.2.3.5. 3-((Pyridin-2-ylmethyl)amino)-4-(4-thiomorpholinophenyl)cyclobut-3-ene-1,2-dione **1e**



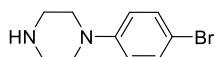
The product **1e** was obtained as a yellow solid. Yield: 85 mg (7%). ¹H NMR (400 MHz, DMSO-*d*₆) δ 9.35 (s, 1H), 8.55 (ddd, *J* = 4.8, 1.8, 0.9 Hz, 1H), 7.94 (d, *J* = 9.0 Hz, 2H), 7.81 (td, *J* = 7.7, 1.8 Hz, 1H), 7.43 (d, *J* = 7.8 Hz, 1H), 7.32 (ddd, *J* = 7.5, 4.8, 1.1 Hz, 1H), 7.03 (d, *J* = 9.1 Hz, 2H), 5.00 (s, 2H), 3.80 – 3.75 (m, 4H), 2.66 – 2.62 (m, 4H). ¹³C NMR (101 MHz, DMSO-*d*₆) δ 153.8, 150.0, 131.5, 117.8, 110.4, 79.0, 47.9, 42.8, 28.0. HRMS: *m/z*: calcd. for C₂₀H₂₀N₃O₂S⁺: 366.1271 [M+H]⁺; found: 366.1274.

4.2.3.6. 3-(4-morpholinophenyl)-4-((pyridin-2-ylmethyl)amino)cyclobut-3-ene-1,2-dione **1h**



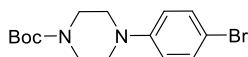
The product **1h** was obtained as a yellow solid. Yield: 86 mg (7%). ¹H NMR (400 MHz, DMSO-*d*₆) δ 9.4 (t, *J* = 6.2 Hz, 1H), 8.6 (ddd, *J* = 4.8, 1.7, 0.9 Hz, 1H), 8.0 (d, *J* = 8.9 Hz, 2H), 7.8 (td, *J* = 7.7, 1.8 Hz, 1H), 7.4 (d, *J* = 7.8 Hz, 1H), 7.3 (ddd, *J* = 7.5, 4.9, 0.9 Hz, 1H), 7.1 (d, *J* = 8.9 Hz, 2H), 5.0 (d, *J* = 6.1 Hz, 2H), 3.8 – 3.7 (m, 4H), 3.3 – 3.3 (m, 4H). ¹³C NMR (101 MHz, DMSO-*d*₆) δ 191.8, 188.9, 178.1, 162.9, 157.4, 152.3, 149.2, 137.0, 128.0, 122.6, 121.6, 119.3, 113.9, 65.8, 48.8, 46.9. HRMS: *m/z*: calcd. for C₂₀H₂₀N₃O₃⁺: 350.1499 [M+H]⁺; found: 350.1497.

4.2.4. 1-(4-Bromophenyl)piperazine **7**



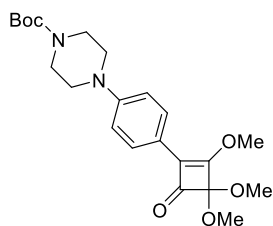
Compound **6** (1.53 ml, 10.00 mmol) was dissolved in DMSO (10 ml) and conc. HBr (10 ml) was added. The reaction mixture was stirred at 60 °C for 1 h. After the reaction was complete, pH was adjusted to 10 with 4M NaOH. This was followed by extraction with EtOAc (3 x 50 ml). Combined organic layers were washed with brine, dried over anhydrous MgSO₄ and evaporated under reduced pressure. Product **7** was obtained as a yellow solid. Yield: 2.1 g (88%). ¹H NMR (400 MHz, DMSO-*d*₆) δ 7.35 – 7.29 (m, 1H), 6.88 – 6.83 (m, 1H), 3.03 – 2.99 (m, 2H), 2.82 – 2.78 (m, 2H). ¹³C NMR (101 MHz, DMSO-*d*₆) δ 150.8, 131.4, 117.1, 109.6, 49.0, 45.4. HRMS: *m/z*: calcd. for C₁₀H₁₄BrN₂⁺: 241.0335 [M+H]⁺; found: 241.0337.

4.2.5. *t*-Butyl 4-(4-bromophenyl)piperazine-1-carboxylate **8A**



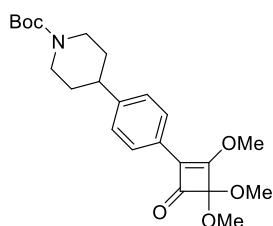
Compound **7** (0.5 g, 2.07 mmol) was dissolved in THF (10 ml) and (Boc)₂O (453 mg; 2.07 mmol) and TEA (578 μl, 4.15 mmol) were added. The reaction mixture was stirred at 60 °C for 3 h. After cooling to rt, water (20 ml) was added, and the reaction mixture was extracted with EtOAc (3 x 30 ml). Combined organic layers were dried over MgSO₄ and evaporated under reduced pressure. The product **8A** was obtained as a yellow solid. Yield: 605 mg (86%). ¹H NMR (400 MHz, DMSO-*d*₆) δ 7.38 – 7.33 (m, 2H), 6.92 – 6.88 (m, 2H), 3.46 – 3.41 (m, 4H), 3.11 – 3.07 (m, 4H), 1.42 (s, 9H). ¹³C NMR (101 MHz, DMSO-*d*₆) δ 153.8, 150.0, 131.5, 117.8, 110.4, 79.0, 47.9, 42.8, 28.0. HRMS: *m/z*: calcd. for C₁₅H₂₂BrN₂O₂⁺: 341.0859 [M+H]⁺; found: 341.0859.

4.2.6. *t*-Butyl 4-(4-(2,3,3-trimethoxy-4-oxocyclobut-1-en-1-yl)phenyl)piperazine-1-carboxylate
10A



Compound **8A** (264 mg, 0.77 mmol) was placed in an annealed two-necked flask with a magnetic stirrer under an argon atmosphere. Next, dry THF (7 ml) was added, and the solution was cooled down to -78 °C. *t*-BuLi (865 μ l, 1.48 mmol) was slowly added as a 1.7M solution in pentane in three portions. After 30 minutes, 3,4-dimethoxycyclobut-3-ene-1,2-dione (100 mg, 0.70 mmol) in THF (1 ml) was added. After another 30 minutes, TFAA (117 μ l, 0.84 mmol) was added, and the mixture was stirred for 20 min. Finally, the reaction was terminated with MeOH (150 μ l, 3.71 mmol) and allowed to warm up to rt. The solvent was evaporated under reduced pressure, and the residue was purified by column chromatography using Hex/EtOAc (2:1). The product was obtained as a yellow solid. Yield: 151 mg (51%). ^1H NMR (400 MHz, DMSO- d_6) δ 7.58 – 7.52 (m, 2H), 7.02 – 6.97 (m, 2H), 4.19 (s, 3H), 3.47 – 3.42 (m, 10H), 3.20 – 3.15 (m, 4H), 1.42 (s, 9H). ^{13}C NMR (101 MHz, DMSO- d_6) δ 189.1, 178.8, 153.8, 150.7, 128.5, 127.7, 117.9, 115.1, 114.7, 79.0, 60.5, 53.2, 47.4, 42.9, 28.0. HRMS: m/z : calcd for $\text{C}_{22}\text{H}_{31}\text{N}_2\text{O}_6^+$: 419.2177 [M+H] $^+$; found: 419.2178.

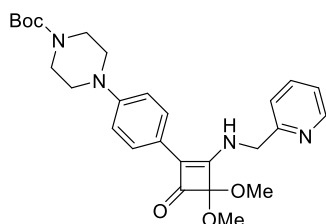
4.2.7. *t*-Butyl 4-(4-(2,3,3-trimethoxy-4-oxocyclobut-1-en-1-yl)phenyl)piperidine-1-carboxylate
10B



Compound **8B** (526 mg, 1.55 mmol) was placed in an annealed two-necked flask with magnetic stirrer under argon atmosphere. Next, dry THF (14 ml) was added and the solution was cooled down to -78 °C. *t*-BuLi (1.73 ml, 2.96 mmol) was slowly added as a 1.7M solution in pentane in three portions. After 30 minutes, 3,4-dimethoxycyclobut-3-ene-1,2-dione (200 mg, 1.41 mmol) in THF (2 ml) was added. After an hour, TFAA (235 μ l, 1.69 mmol) was added and the mixture was stirred for 20 min. Finally, the reaction was terminated with MeOH (300 μ l, 7.41 mmol) and allowed to warm up to rt. The solvent was evaporated under reduced pressure and the residue was purified by column chromatography using Hex/EtOAc (3:1). The product was obtained as a pale oil. Yield: 141 mg (24%). ^1H NMR (400 MHz, DMSO- d_6) δ 7.61 (d, J = 8.2

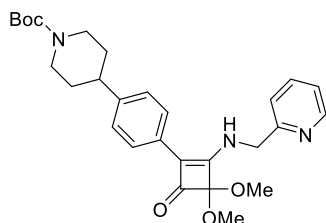
Hz, 2H), 7.33 (d, $J = 8.2$ Hz, 2H), 4.22 (s, 3H), 4.07 (d, $J = 12.1$ Hz, 2H), 3.46 (s, 6H), 2.80 (br s, 2H), 2.69 (tt, $J = 12.2, 3.3$ Hz, 1H), 1.73 (d, $J = 12.8$ Hz, 2H), 1.53 – 1.44 (m, 2H), 1.41 (s, 9H). ^{13}C NMR (126 MHz, $\text{DMSO-}d_6$) δ 189.1, 180.8, 153.8, 146.7, 127.9, 127.3, 126.7, 125.5, 114.7, 78.6, 60.8, 53.3, 43.8, 41.6, 32.5, 28.1. HRMS: m/z calcd. for $\text{C}_{23}\text{H}_{32}\text{NO}_6^+$: 418.2224 $[\text{M}+\text{H}]^+$; found: 418.2222.

4.2.8. *t*-Butyl 4-(4-(3,3-dimethoxy-4-oxo-2-((pyridin-2-ylmethyl)amino)cyclobut-1-en-1-yl)phenyl)-piperazine-1-carboxylate **11A**



Compound **10A** (80 mg, 0.19 mmol) was dissolved in MeCN (4 ml) followed by addition of 2-(aminomethyl)pyridine (20 μl , 0.19 mmol). The reaction mixture was stirred at rt for 16 h. After the reaction was completed, the solvent was evaporated under reduced pressure and the residue was purified by column chromatography using DCM/MeOH (95:5). The product was obtained as a brown oil. Yield: 90 mg (95%). ^1H NMR (400 MHz, $\text{DMSO-}d_6$) δ 8.94 (t, $J = 6.1$ Hz, 1H), 8.56 (d, $J = 4.6$ Hz, 1H), 7.83 (td, $J = 7.7, 1.6$ Hz, 1H), 7.67 (d, $J = 8.7$ Hz, 2H), 7.44 (d, $J = 7.8$ Hz, 1H), 7.33 (dd, $J = 7.0, 5.2$ Hz, 1H), 6.96 (d, $J = 8.8$ Hz, 2H), 4.68 (d, $J = 6.2$ Hz, 2H), 3.48 – 3.43 (m, 4H), 3.33 (s, 6H), 3.16 – 3.09 (m, 4H), 1.42 (s, 9H). ^{13}C NMR (101 MHz, $\text{DMSO-}d_6$) δ 185.4, 166.6, 157.6, 153.8, 149.4, 148.9, 136.8, 126.6, 122.5, 121.3, 121.3, 120.1, 115.5, 114.1, 79.0, 52.9, 49.8, 48.0, 43.0, 28.0. HRMS: m/z : calcd. for $\text{C}_{27}\text{H}_{33}\text{N}_4\text{O}_5^-$: 493.2456 $[\text{M}-\text{H}]^-$; found: 493.2457.

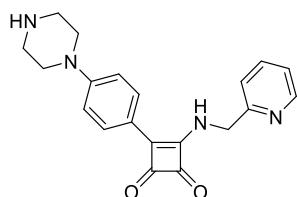
4.2.9. *t*-Butyl 4-(4-(3,3-dimethoxy-4-oxo-2-((pyridin-2-ylmethyl)amino)cyclobut-1-en-1-yl)phenyl)-piperidine-1-carboxylate **11B**



Compound **10B** (141 mg, 0.34 mmol) was dissolved in MeCN (2 ml) followed by addition of 2-(aminomethyl)pyridine (35 μl , 0.34 mmol). The reaction mixture was stirred at rt for 16 h. After the reaction was completed, the solvent was evaporated under reduced pressure and the residue was purified by column chromatography using DCM/MeOH (95:5). The product was obtained as a yellow solid. Yield: 124 mg (74%). ^1H NMR (400 MHz, $\text{DMSO-}d_6$) δ 9.10 (t, $J =$

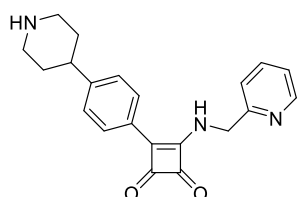
6.2 Hz, 1H), 8.58 – 8.53 (m, 1H), 7.82 (td, $J = 7.7, 1.8$ Hz, 1H), 7.71 (d, $J = 8.2$ Hz, 2H), 7.43 (d, $J = 7.8$ Hz, 1H), 7.32 (dd, $J = 6.8, 5.0$ Hz, 1H), 7.26 (d, $J = 8.2$ Hz, 2H), 4.69 (d, $J = 6.2$ Hz, 2H), 4.07 (d, $J = 11.1$ Hz, 2H), 3.34 (s, 6H), 2.79 (s, 2H), 2.67 (tt, $J = 11.7, 3.0$ Hz, 1H), 1.73 (d, $J = 13.9$ Hz, 2H), 1.50 (td, $J = 12.6, 4.1$ Hz, 2H), 1.41 (s, 9H). ^{13}C NMR (126 MHz, $\text{DMSO-}d_6$) δ 185.6, 167.7, 157.4, 153.8, 148.9, 144.3, 136.8, 128.1, 126.8, 125.6, 122.5, 121.3, 119.5, 114.1, 78.5, 52.9, 49.8, 43.8, 41.5, 32.7, 28.1. HRMS: m/z calcd. for $\text{C}_{28}\text{H}_{34}\text{N}_3\text{O}_5^-$: 492.2504 [M-H] $^-$; found: 492.2505.

4.2.10. 3-(4-(Piperazin-1-yl)phenyl)-4-((pyridin-2-ylmethyl)amino)cyclobut-3-ene-1,2-dione **1f**



Compound **11A** (80 mg; 0.16 mmol) was dissolved in DCM (1 ml). Next, 10% HCl (1 ml) was added, and the biphasic mixture was stirred at rt for 15 min. The aqueous layer was separated, and pH was adjusted to 9 with 1M NaOH. The precipitated solid was filtered and washed with small amount of cold water. The product was obtained as a yellow solid. Yield: 41 mg (73%). ^1H NMR (400 MHz, $\text{DMSO-}d_6$) δ 9.58 (br s, 1H), 8.56 – 8.52 (m, 1H), 7.98 (d, $J = 8.9$ Hz, 2H), 7.80 (td, $J = 7.7, 1.8$ Hz, 1H), 7.43 (d, $J = 7.9$ Hz, 1H), 7.30 (ddd, $J = 7.5, 4.9, 0.9$ Hz, 1H), 7.01 (d, $J = 8.9$ Hz, 2H), 4.99 (s, 2H), 3.25 – 3.20 (m, 4H), 2.85 – 2.77 (m, 4H). ^{13}C NMR (101 MHz, $\text{DMSO-}d_6$) δ 191.8, 189.0, 177.8, 163.1, 157.6, 152.6, 149.2, 137.0, 128.1, 122.5, 121.5, 118.7, 113.8, 48.7, 47.8, 45.4. HRMS: m/z : calcd. for $\text{C}_{20}\text{H}_{21}\text{N}_4\text{O}_2^+$: 349.1659 [M+H] $^+$; found: 349.1650.

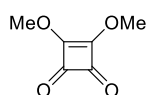
4.2.11. 3-(4-(Piperidin-4-yl)phenyl)-4-((pyridin-2-ylmethyl)amino)cyclobut-3-ene-1,2-dione **1g**



Compound **11B** (107 mg, 0.22 mmol) was dissolved in 10% HCl (1 ml) and stirred at rt for 15 min. The pH of the reaction mixture was adjusted to 9 with 1M NaOH. The precipitated solid was filtered and dissolved in DCM (1 ml). Consequently, the obtained product was dissolved in TFA (1 ml), and the mixture was stirred at rt for 2 hours. After that, the solvent was evaporated under reduced pressure, and the residue was washed with saturated NaHCO_3 . The precipitated solid was filtered, washed with a small amount of cold water and dried under a vacuum. The product was obtained as a light orange solid. Yield: 21 mg (28%). ^1H NMR (400

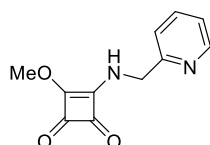
MHz, DMSO- d_6) δ 8.56 – 8.52 (m, 1H), 8.05 (d, J = 8.2 Hz, 2H), 7.80 (td, J = 7.7, 1.8 Hz, 1H), 7.45 (d, J = 7.9 Hz, 1H), 7.40 (d, J = 8.3 Hz, 2H), 7.34 – 7.28 (m, 1H), 5.01 (s, 2H), 3.32 (d, J = 12.4 Hz, 2H), 2.99 – 2.84 (m, 3H), 1.95 – 1.81 (m, 4H). ^{13}C NMR (101 MHz, DMSO- d_6) δ 193.2, 188.9, 179.1, 161.7, 157.1, 149.2, 147.7, 137.0, 127.5, 127.2, 126.6, 122.7, 121.6, 48.8, 43.6, 29.5. HRMS: m/z calcd. for $\text{C}_{21}\text{H}_{22}\text{N}_3\text{O}_2^+$: 348.1707 [M+H] $^+$; found: 348.1706.

4.2.12. 3,4-Dimethoxycyclobut-3-ene-1,2-dione **12**



Squaric acid **3** (2.053 g; 18 mmol) was suspended in dry MeOH (18 ml), and trimethyl orthoformate was added (4 ml; 36.5 mmol). The reaction mixture was stirred under reflux at 65 °C for 24 hours. After the reaction was completed (monitoring by TLC), the reaction mixture was evaporated under reduced pressure with a small amount of SiO_2 . The product was purified by column chromatography using Hex/EtOAc (1:2). The product was obtained as a white solid. Yield: 2.558 g (89%). The analytical data correspond with the literature [30].

4.2.13. 3-Methoxy-4-((pyridin-2-ylmethyl)amino)cyclobut-3-ene-1,2-dione **13**



Dimethoxy derivate **12** (1.84 g; 13 mmol) was dissolved in MeCN (15 ml). Into the solution, 2-(aminomethyl)pyridine (1.33 ml; 13 mmol) was added dropwisely. After the addition, the reaction mixture was stirred at rt for 40 min. The formed precipitate was filtered, obtained solid was washed with MeCN and subsequently freeze-dried. The product was obtained as a white solid. Yield: 2.25 g (80%). ^1H NMR (400 MHz, DMSO- d_6) δ 8.94 (br s, 1H), 8.54 (d, J = 4.7 Hz, 1H), 7.79 (td, J = 7.7, 1.8 Hz, 1H), 7.36 (d, J = 7.8 Hz, 1H), 7.30 (ddd, J = 7.7, 4.8, 1.1 Hz, 1H), 4.69 (br s, 2H), 4.28 (s, 3H). ^{13}C NMR (101 MHz, DMSO- d_6) δ 189.0, 182.5, 177.3, 172.52, 156.9, 148.8, 136.6, 122.2, 121.1, 59.7, 48.4. HRMS: m/z calcd. for $\text{C}_{11}\text{H}_{11}\text{N}_2\text{O}_3^+$: 219.0764 [M+H] $^+$; found: 219.0765

4.2.14. General procedure for the synthesis of **2**

Method A:

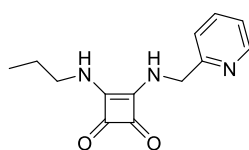
Precursor **13** (200 mg; 0.916 mmol) was dissolved in MeCN (10 ml) and amine (0.916 mmol) was added. The reaction mixture was stirred at rt or 50 °C (for derivative **2c**, **2g**, **2j**) for 24 h. The formed precipitate was filtered, and the solid was washed with MeCN. The product was

purified by column chromatography using DCM/MeOH (9:1) or Hex/EtOAc (6:4), and freeze-dried.

Method B:

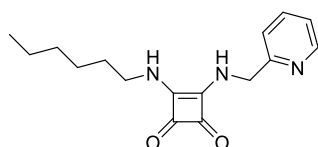
Precursor **13** (200 mg; 0.916 mmol) was dissolved in MeCN (10 ml) and benzoxazolamine (0.916 mmol) with DBU (0.916 mmol) were added. The reaction mixture was stirred at 50 °C for 24 h. After the reaction was complete, the solvent was evaporated under reduced pressure. The product was isolated by filtration of evaporated residue through a small column of silica (SiO₂) using 2% solution of MeOH in DCM as eluent. The product was isolated by crystallization from obtained eluents.

4.2.14.1. 3-(Propylamino)-4-((pyridin-2-ylmethyl)amino)cyclobut-3-ene-1,2-dione **2a**



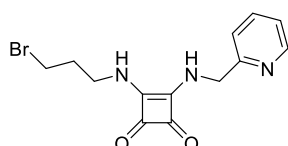
Prepared by *Method A* as white solid. Yield: 154.7 mg (69%). ¹H NMR (400 MHz, DMSO-*d*₆) δ 8.59 – 8.54 (m, 1H), 7.90 (br s, 1H), 7.81 (td, *J* = 7.7, 1.8 Hz, 1H), 7.54 (br s, 1H), 7.37 (d, *J* = 7.8 Hz, 1H), 7.35 – 7.30 (m, 1H), 4.83 (d, *J* = 5.3 Hz, 2H), 3.47 (d, *J* = 5.6 Hz, 2H), 1.59 – 1.48 (sxt, *J* = 7.1 Hz, 2H), 0.88 (t, *J* = 7.4 Hz, 3H). ¹³C NMR (101 MHz, DMSO-*d*₆) δ 182.8, 182.4, 168.1, 167.5, 157.6, 149.2, 137.2, 122.64, 121.6, 48.2, 45.0, 24.0, 10.8. HRMS: *m/z* calcd. for C₁₃H₁₆N₃O₂⁺: 246.1237 [M+H]⁺; found: 246.1235.

4.2.14.2. 3-(Hexylamino)-4-((pyridin-2-ylmethyl)amino)cyclobut-3-ene-1,2-dione **2b**



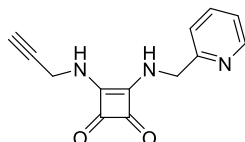
Prepared by *Method A* as white solid. Yield: 167.4 mg (64%). ¹H NMR (400 MHz, DMSO-*d*₆) δ 8.56 (d, *J* = 4.4 Hz, 1H), 7.89 (br s, 1H), 7.81 (td, *J* = 7.7, 1.8 Hz, 1H), 7.50 (br s, 1H), 7.37 (d, *J* = 7.8 Hz, 1H), 7.35 – 7.30 (m, 1H), 4.82 (d, *J* = 4.9 Hz, 2H), 3.51 (d, *J* = 4.7 Hz, 2H), 1.56 – 1.46 (m, 2H), 1.34 – 1.23 (m, 6H), 0.88 – 0.82 (m, 3H). ¹³C NMR (101 MHz, DMSO-*d*₆) δ 182.8, 182.4, 168.0, 167.5, 157.5, 149.1, 137.1, 122.6, 121.6, 48.2, 43.3, 30.8, 30.6, 25.5, 22.0, 13.9. HRMS: *m/z*: calcd. for C₁₆H₂₂N₃O₂⁺: 288.1707 [M+H]⁺; found: 288.1706.

4.2.14.3. 3-((3-Bromopropyl)amino)-4-((pyridin-2-ylmethyl)amino)cyclobut-3-ene-1,2-dione **2c**



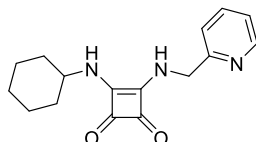
Prepared by *Method A* as white solid. Yield: 59.7 mg (20%). ^1H NMR (400 MHz, $\text{DMSO-}d_6$) δ 8.56 (ddd, $J = 4.8, 1.5, 0.8$ Hz, 1H), 8.01 (br s, 1H), 7.81 (td, $J = 7.7, 1.8$ Hz, 1H), 7.70 (br s, 1H), 7.38 (d, $J = 7.8$ Hz, 1H), 7.32 (ddd, $J = 7.5, 4.9, 0.9$ Hz, 1H), 4.82 (d, $J = 4.9$ Hz, 2H), 3.62 (dd, $J = 12.5, 6.2$ Hz, 2H), 3.56 (t, $J = 6.6$ Hz, 2H), 2.12 – 2.04 (m, 2H). ^{13}C NMR (101 MHz, $\text{DMSO-}d_6$) δ 182.7, 182.6, 167.9, 167.8, 160.0, 149.1, 137.1, 122.6, 121.6, 48.2, 41.8, 33.6, 31.5. HRMS: m/z : calcd. for $\text{C}_{13}\text{H}_{15}\text{BrN}_3\text{O}_2^+$: 324.0342 $[\text{M}+\text{H}]^+$; found: 324.0340.

4.2.14.4. 3-(Prop-2-yn-1-ylamino)-4-((pyridin-2-ylmethyl)amino)cyclobut-3-ene-1,2-dione **2d**



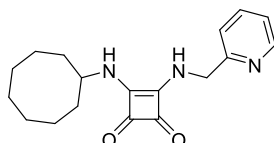
Prepared by *Method A* as white solid. Yield: 67.7 mg (33%). ^1H NMR (400 MHz, $\text{DMSO-}d_6$) δ 8.57 (ddd, $J = 4.8, 1.7, 0.9$ Hz, 1H), 8.00 (br s, 1H), 7.81 (td, $J = 7.7, 1.8$ Hz, 2H), 7.37 (d, $J = 7.8$ Hz, 1H), 7.32 (ddd, $J = 7.5, 4.9, 1.1$ Hz, 1H), 4.82 (d, $J = 4.0$ Hz, 2H), 4.37 (dd, $J = 5.8, 2.2$ Hz, 2H), 3.36 (t, $J = 2.5$ Hz, 1H). ^{13}C NMR (101 MHz, $\text{DMSO-}d_6$) δ 183.6, 183.1, 168.5, 167.7, 158.0, 149.7, 137.7, 123.2, 122.1, 81.2, 75.7, 48.8, 33.3. HRMS: m/z : calcd. for $\text{C}_{13}\text{H}_{12}\text{N}_3\text{O}_2^+$: 242.0924 $[\text{M}+\text{H}]^+$; found: 242.0925.

4.2.14.5. 3-(Cyclohexylamino)-4-((pyridin-2-ylmethyl)amino)cyclobut-3-ene-1,2-dione **2e**



Prepared by *Method A* as white solid. Yield: 173.2 mg (69%). ^1H NMR (400 MHz, $\text{DMSO-}d_6$) δ 8.57 (d, $J = 4.5$ Hz, 1H), 7.82 (td, $J = 7.7, 1.8$ Hz, 2H – overlapped with -NH-), 7.55 (br s, 1H), 7.38 (d, $J = 7.8$ Hz, 1H), 7.33 (dd, $J = 7.1, 5.0$ Hz, 1H), 4.83 (d, $J = 5.1$ Hz, 2H), 3.79 (br s, 1H), 1.92 – 1.83 (m, 2H), 1.72 – 1.64 (m, 2H), 1.58 – 1.50 (m, 1H), 1.37 – 1.23 (m, 4H), 1.22 – 1.13 (m, 1H). ^{13}C NMR (101 MHz, $\text{DMSO-}d_6$) δ 182.5, 182.3, 167.5, 167.2, 157.5, 149.1, 137.1, 122.6, 121.6, 52.0, 48.2, 33.7, 24.8, 23.9. HRMS: m/z : calcd. for $\text{C}_{16}\text{H}_{20}\text{N}_3\text{O}_2^+$: 286.1550 $[\text{M}+\text{H}]^+$; found: 286.1548.

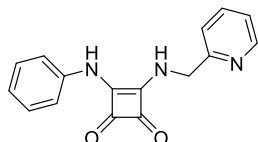
4.2.14.6. 3-(Cyclooctylamino)-4-((pyridin-2-ylmethyl)amino)cyclobut-3-ene-1,2-dione **2f**



Prepared by *Method A* as white solid. Yield: 220.6 mg (77%). ^1H NMR (400 MHz, $\text{DMSO-}d_6$) δ 8.57 (d, $J = 4.7$ Hz, 1H), 7.82 (td, $J = 7.7, 1.7$ Hz, 2H – overlapped with -NH-), 7.56 (br s, 1H),

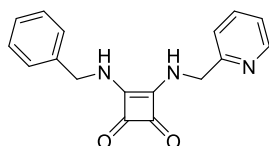
7.38 (d, $J = 7.8$ Hz, 1H), 7.33 (dd, $J = 7.3, 5.0$ Hz, 1H), 4.83 (d, $J = 5.4$ Hz, 2H), 4.08 (br s, 1H), 1.92 – 1.80 (m, 2H), 1.68 – 1.44 (m, 12H). ^{13}C NMR (101 MHz, $\text{DMSO-}d_6$) δ 182.6, 182.3, 167.6, 167.0, 157.4, 149.1, 137.1, 122.6, 121.7, 53.2, 48.2, 32.5, 26.8, 24.9, 22.6. HRMS: m/z : calcd. for $\text{C}_{18}\text{H}_{24}\text{N}_3\text{O}_2^+$: 314.1863 $[\text{M}+\text{H}]^+$; found: 314.1861.

4.2.14.7. 3-(Phenylamino)-4-((pyridin-2-ylmethyl)amino)cyclobut-3-ene-1,2-dione **2g**



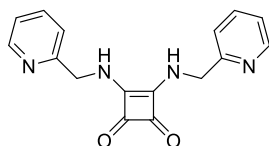
Prepared by *Method A* as white solid. Yield: 122.2 mg (48%). ^1H NMR (400 MHz, $\text{DMSO-}d_6$) δ 9.84 (br s, 1H), 8.60 (d, $J = 4.5$ Hz, 1H), 8.21 (br s, 1H), 7.84 (td, $J = 7.7, 1.5$ Hz, 1H), 7.44 (t, $J = 7.3$ Hz, 3H), 7.38 – 7.29 (m, 3H), 7.03 (t, $J = 7.3$ Hz, 1H), 4.94 (d, $J = 5.0$ Hz, 2H). ^{13}C NMR (101 MHz, $\text{DMSO-}d_6$) δ 184.1, 180.6, 169.1, 163.8, 156.9, 149.2, 139.0, 137.2, 129.3, 122.8, 122.6, 121.7, 118.0, 48.5. HRMS: m/z : calcd. for $\text{C}_{16}\text{H}_{14}\text{N}_3\text{O}_2^+$: 280.1081 $[\text{M}+\text{H}]^+$; found: 280.1080.

4.2.14.8. 3-(Benzylamino)-4-((pyridin-2-ylmethyl)amino)cyclobut-3-ene-1,2-dione **2h**



Prepared by *Method A* as white solid. Yield: 228.1 mg (85%). ^1H NMR (400 MHz, $\text{DMSO-}d_6$) δ 8.55 (d, $J = 4.4$ Hz, 1H), 7.91 (br s, 1H), 7.80 (td, $J = 5.89, 1.60$ Hz, 1H), 7.41 – 7.26 (m, 8H), 4.83 (s, 2H), 4.73 (d, $J = 6.0$ Hz, 2H). ^{13}C NMR (101 MHz, $\text{DMSO-}d_6$) δ 182.9, 182.7, 167.8, 167.6, 157.5, 149.1, 138.9, 137.1, 128.6, 127.5, 127.4, 122.6, 121.6, 48.2, 46.8. HRMS: m/z : calcd. for $\text{C}_{17}\text{H}_{16}\text{N}_3\text{O}_2^+$: 294.1237 $[\text{M}+\text{H}]^+$; found: 294.1236.

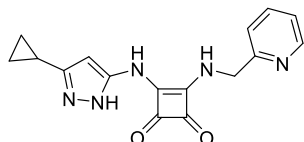
4.2.14.9. 3,4-Bis((pyridin-2-ylmethyl)amino)cyclobut-3-ene-1,2-dione **2i**



Precursor **2** (200 mg; 1.41 mmol) was dissolved in MeOH (10 ml) and 2-(aminomethyl)pyridine was added (290 μl ; 2.82 mmol). Reaction mixture was stirred for 3 hours at 50 $^\circ\text{C}$. After the reaction was complete, the solvent was evaporated under reduced pressure and the product was purified by column chromatography using DCM/MeOH (9:1). The product was obtained as white solid. Yield: 269.7 mg (65%). ^1H NMR (400 MHz, $\text{DMSO-}d_6$) δ 9.35 (d, $J = 6.7$ Hz, 2H), 8.54 (d, $J = 4.4$ Hz, 2H), 7.80 (td, $J = 7.7, 1.7$ Hz, 2H), 7.37 (d, $J = 7.8$ Hz, 2H), 7.31 (dd,

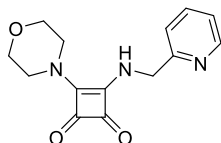
$J = 7.0, 5.2$ Hz, 2H), 4.85 (d, $J = 6.4$ Hz, 4H). ^{13}C NMR (101 MHz, $\text{DMSO-}d_6$) δ 178.8, 168.9, 157.4, 149.1, 137.0, 122.6, 121.5, 48.3. HRMS: m/z : calcd. for $\text{C}_{16}\text{H}_{15}\text{N}_4\text{O}_2^+$: 295.1190 $[\text{M}+\text{H}]^+$; found: 295.1188.

4.2.14.10. 3-((3-Cyclopropyl-1H-pyrazol-5-yl)amino)-4-((pyridin-2-ylmethyl)amino)cyclobut-3-ene-1,2-dione **2j**



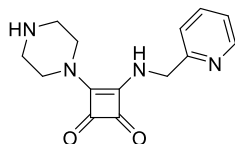
Prepared by *Method A* as white solid. Yield: 134.6 mg (48%). ^1H NMR (400 MHz, $\text{DMSO-}d_6$) δ 12.20 (s, 1H), 10.48 (br s, 1H), 8.86 (br s, 1H), 8.63 – 8.51 (m, 1H), 7.81 (td, $J = 7.7, 1.8$ Hz, 1H), 7.40 (d, $J = 7.8$ Hz, 1H), 7.32 (dd, $J = 6.9, 5.1$ Hz, 1H), 5.69 (br s, 1H), 4.94 (d, $J = 6.3$ Hz, 2H), 1.89 – 1.81 (m, 1H), 0.99 – 0.87 (m, 2H), 0.74 – 0.61 (m, 2H). ^{13}C NMR (101 MHz, $\text{DMSO-}d_6$) δ 184.3, 168.5, 163.6, 157.4, 149.3, 148.2, 147.6, 137.1, 132.1, 122.6, 121.4, 90.4, 48.1, 7.9, 6.6. HRMS: m/z : calcd. for $\text{C}_{16}\text{H}_{16}\text{N}_5\text{O}_2^+$: 310.1299 $[\text{M}+\text{H}]^+$; found: 310.1300.

4.2.14.11. 3-Morpholino-4-((pyridin-2-ylmethyl)amino)cyclobut-3-ene-1,2-dione **2k**



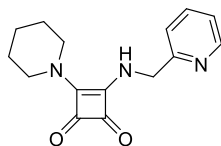
Prepared by *Method A* as white solid. Yield: 81.3 mg (33%). ^1H NMR (500 MHz, $\text{DMSO-}d_6$) δ 8.54 (ddd, $J = 4.8, 1.7, 0.9$ Hz, 1H), 8.29 (t, $J = 6.2$ Hz, 1H), 7.80 (td, $J = 7.7, 1.8$ Hz, 1H), 7.40 (d, $J = 7.8$ Hz, 1H), 7.30 (ddd, $J = 7.5, 4.9, 1.0$ Hz, 1H), 4.88 (d, $J = 6.3$ Hz, 2H), 3.70 (s, 8H). ^{13}C NMR (101 MHz, $\text{DMSO-}d_6$) δ 182.7, 182.6, 167.0, 166.1, 158.2, 149.1, 136.9, 122.4, 121.4, 65.9, 48.3, 46.8. HRMS: m/z : calcd. for $\text{C}_{14}\text{H}_{16}\text{N}_3\text{O}_3^+$: 274.1186 $[\text{M}+\text{H}]^+$; found: 274.1184.

4.2.14.12. 3-(Piperazin-1-yl)-4-((pyridin-2-ylmethyl)amino)cyclobut-3-ene-1,2-dione **2l**



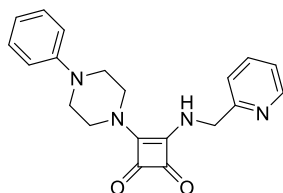
Prepared by *Method A* as white solid. Yield: 170.1 mg (68%). ^1H NMR (500 MHz, $\text{DMSO-}d_6$) δ 8.54 (ddd, $J = 4.8, 1.6, 0.9$ Hz, 1H), 8.22 (t, $J = 5.9$ Hz, 1H), 7.83 – 7.77 (m, 1H), 7.38 (d, $J = 7.7$ Hz, 1H), 7.29 (ddd, $J = 7.4, 4.9, 0.9$ Hz, 1H), 4.89 (d, $J = 6.0$ Hz, 2H), 3.83 (s, 1H), 3.61 (s, 4H), 2.79 – 2.74 (m, 4H). ^{13}C NMR (126 MHz, $\text{DMSO-}d_6$) δ 182.8, 182.2, 166.8, 166.1, 158.4, 149.1, 136.9, 122.4, 121.3, 48.3, 47.9, 45.6. HRMS: m/z : calcd. for $\text{C}_{14}\text{H}_{17}\text{N}_4\text{O}_2^+$: 273.1346 $[\text{M}+\text{H}]^+$; found: 273.1344.

4.2.14.13. 3-(Piperidin-1-yl)-4-((pyridin-2-ylmethyl)amino)cyclobut-3-ene-1,2-dione **2m**



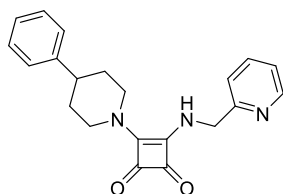
Prepared by *Method A* as white solid. Yield: 178.7 mg (72%). ^1H NMR (400 MHz, $\text{DMSO-}d_6$) δ 8.57 – 8.50 (m, 1H), 8.22 (t, $J = 5.8$ Hz, 1H), 7.85 – 7.75 (m, 1H), 7.38 (d, $J = 7.8$ Hz, 1H), 7.33 – 7.26 (m, 1H), 4.89 (d, $J = 6.2$ Hz, 2H), 3.66 (s, 4H), 1.60 (s, 6H). ^{13}C NMR (101 MHz, $\text{DMSO-}d_6$) δ 183.4, 182.6, 167.3, 166.8, 159.0, 149.6, 137.5, 122.9, 121.8, 48.9, 48.1, 26.2, 23.7. HRMS: m/z : calcd. for $\text{C}_{15}\text{H}_{18}\text{N}_3\text{O}_2^+$: 272.1394 $[\text{M}+\text{H}]^+$; found: 272.1393.

4.2.14.14. 3-(4-Phenylpiperazin-1-yl)-4-((pyridin-2-ylmethyl)amino)cyclobut-3-ene-1,2-dione **2n**



Prepared by *Method A* as white solid. Yield: 268.3 mg (84%). ^1H NMR (400 MHz, $\text{DMSO-}d_6$) δ 8.55 (ddd, $J = 4.9, 1.7, 0.9$ Hz, 1H), 8.38 (t, $J = 6.0$ Hz, 1H), 7.80 (td, $J = 7.7, 1.8$ Hz, 1H), 7.41 (d, $J = 7.9$ Hz, 1H), 7.30 (ddd, $J = 7.6, 4.9, 1.0$ Hz, 1H), 7.27 – 7.19 (m, 2H), 7.04 – 6.97 (m, 2H), 6.83 (t, $J = 7.2$ Hz, 1H), 4.91 (d, $J = 6.0$ Hz, 2H), 3.85 (s, 4H), 3.28 – 3.22 (m, 4H). ^{13}C NMR (101 MHz, $\text{DMSO-}d_6$) δ 182.7, 182.6, 167.1, 166.0, 158.3, 150.7, 149.1, 136.9, 129.0, 122.4, 121.4, 119.6, 116.1, 48.5, 48.4, 46.4. HRMS: m/z : calcd. for $\text{C}_{20}\text{H}_{21}\text{N}_4\text{O}_2^+$: 349.1659 $[\text{M}+\text{H}]^+$; found: 349.1660.

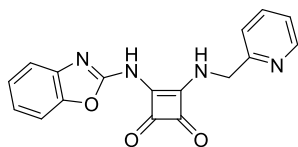
4.2.14.15. 3-(4-Phenylpiperidin-1-yl)-4-((pyridin-2-ylmethyl)amino)cyclobut-3-ene-1,2-dione **2o**



Prepared by *Method A* as white solid. Yield: 227.5 mg (71%). ^1H NMR (500 MHz, $\text{DMSO-}d_6$) δ 8.54 (ddd, $J = 4.8, 1.9, 1.0$ Hz, 1H), 8.29 (t, $J = 6.3$ Hz, 1H), 7.81 (td, $J = 7.7, 1.8$ Hz, 1H), 7.41 (dt, $J = 7.8, 1.1$ Hz, 1H), 7.35 – 7.25 (m, 5H), 7.23 – 7.18 (m, 1H), 4.91 (d, $J = 6.2$ Hz, 2H), 4.41 (br s, 2H), 3.24 (td, $J = 12.7, 2.9$ Hz, 2H), 2.81 (tt, $J = 11.9, 3.8$ Hz, 1H), 1.88 – 1.67 (m, 4H). ^{13}C NMR (126 MHz, $\text{DMSO-}d_6$) δ 183.4, 182.8, 167.5, 166.8, 159.0, 149.6, 145.9, 137.5,

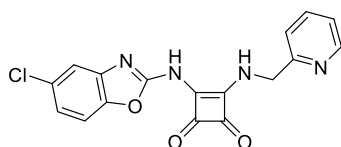
129.0, 127.3, 126.8, 122.9, 121.9, 48.9, 47.8, 41.1, 33.4. HRMS: m/z : calcd. for $C_{21}H_{22}N_3O_2^+$: 348.1707 $[M+H]^+$; found: 348.1700.

4.2.14.16. **3-(Benzo[d]oxazol-2-ylamino)-4-((pyridin-2-ylmethyl)amino)cyclobut-3-ene-1,2-dione *2p***



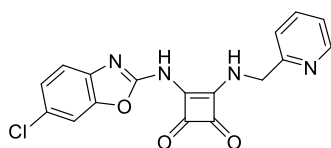
Prepared by *Method B* as white solid. Yield: 108.7 mg (50%). 1H NMR (400 MHz, DMSO- d_6) δ 12.52 (br s, 1H), 9.50 (br s, 1H), 8.64 (d, $J = 4.6$ Hz, 1H), 7.84 (td, $J = 7.7, 1.8$ Hz, 1H), 7.58 (d, $J = 7.9$ Hz, 1H), 7.54 (d, $J = 7.7$ Hz, 1H), 7.48 (d, $J = 7.8$ Hz, 1H), 7.37 – 7.34 (m, 1H), 7.33 – 7.29 (m, 1H), 7.24 (td, $J = 7.8, 1.2$ Hz, 1H), 5.03 (d, $J = 6.0$ Hz, 2H). ^{13}C NMR (101 MHz, DMSO- d_6) δ 187.8, 181.6, 171.1, 170.9, 160.3, 156.8, 156.3, 149.1, 148.0, 140.3, 137.1, 124.8, 123.2, 122.6, 121.4, 110.0, 48.0. HRMS: m/z : calcd. for $C_{17}H_{13}N_4O_3^+$: 321.0982 $[M + H]^+$; found: 321.0979.

4.2.14.17. **3-((5-Chlorobenzo[d]oxazol-2-yl)amino)-4-((pyridin-2-ylmethyl)amino)cyclobut-3-ene-1,2-dione *2q***



Prepared by *Method B* as white solid. Yield: 179.4 mg (47%). 1H NMR (400 MHz, DMSO- d_6) δ 12.67 (br s, 1H), 9.33 (t, $J = 6.2$ Hz, 1H), 8.61 – 8.58 (m, 1H), 7.83 (td, $J = 7.7, 1.8$ Hz, 1H), 7.61 (d, $J = 8.6$ Hz, 1H), 7.59 (d, $J = 2.1$ Hz, 1H), 7.46 (d, $J = 7.8$ Hz, 1H), 7.34 (ddd, $J = 12.2, 4.9, 0.7$ Hz, 1H), 7.26 (dd, $J = 8.6, 2.2$ Hz, 1H), 5.01 (d, $J = 6.2$ Hz, 2H). ^{13}C NMR (101 MHz, DMSO- d_6) δ 188.0, 181.6, 171.1, 160.0, 157.4, 157.1, 149.0, 147.0, 141.8, 137.1, 128.8, 122.8, 122.6, 121.3, 117.1, 111.3, 48.1. HRMS: m/z : calcd. for $C_{17}H_{12}ClN_4O_3^+$: 355.0592 $[M+H]^+$; found: 355.0592.

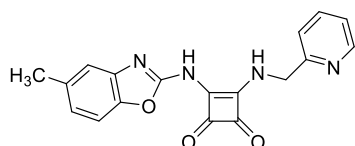
4.2.14.18. **3-((6-Chlorobenzo[d]oxazol-2-yl)amino)-4-((pyridin-2-ylmethyl)amino)cyclobut-3-ene-1,2-dione *2r***



Prepared by *Method B* as white solid. Yield: 105.2 mg (36%). 1H NMR (400 MHz, DMSO- d_6) δ 12.62 (br s, 1H), 9.40 (t, $J = 5.9$ Hz, 1H), 8.67 – 8.59 (m, 1H), 7.83 (td, $J = 7.7, 1.8$ Hz, 1H),

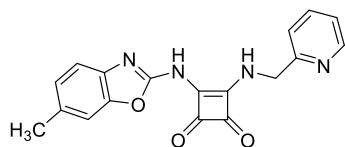
7.78 (d, $J = 1.9$ Hz, 1H), 7.51 (d, $J = 8.4$ Hz, 1H), 7.47 (d, $J = 7.9$ Hz, 1H), 7.36 (d, $J = 1.8$ Hz, 1H), 7.35 – 7.31 (m, 1H), 5.02 (d, $J = 6.0$ Hz, 2H). ^{13}C NMR (101 MHz, $\text{DMSO-}d_6$) δ 187.9, 181.5, 171.0, 160.0, 157.2 156.8, 149.1, 148.4, 139.5, 137.1, 127.0, 125.0, 122.6, 121.4, 118.2, 110.7, 48.1. HRMS: m/z : calcd. for $\text{C}_{17}\text{H}_{12}\text{ClN}_4\text{O}_3^+$: 355.0592 $[\text{M}+\text{H}]^+$; found: 355.0592.

4.2.14.19. 3-((5-Methylbenzo[d]oxazol-2-yl)amino)-4-((pyridin-2-ylmethyl)amino)cyclobut-3-ene-1,2-dione **2s**



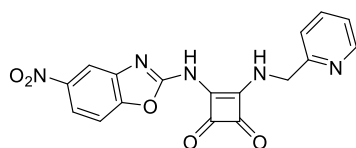
Prepared by *Method B* as white solid. Yield: 64.4 mg (21%). ^1H NMR (400 MHz, $\text{DMSO-}d_6$) δ 12.48 (br s, 1H), 9.49 (br s, 1H), 8.63 (d, $J = 4.3$ Hz, 1H), 7.84 (td, $J = 7.7, 1.7$ Hz, 1H), 7.46 (t, $J = 8.8$ Hz, 2H), 7.38 – 7.29 (m, 2H), 7.07 – 6.99 (m, 1H), 5.02 (d, $J = 5.9$ Hz, 2H), 2.39 (s, 3H). ^{13}C NMR (101 MHz, $\text{DMSO-}d_6$) δ 187.7, 181.1, 170.7, 163.7, 156.9, 156.3, 149.1, 148.5, 137.1, 134.1, 131.5 123.8, 122.6, 121.4, 114.8, 109.5, 48.1, 21.0. HRMS: m/z : calcd. for $\text{C}_{18}\text{H}_{15}\text{N}_4\text{O}_3^+$: 335.1139 $[\text{M}+\text{H}]^+$; found: 335.1137.

4.2.14.20. 3-((6-Methylbenzo[d]oxazol-2-yl)amino)-4-((pyridin-2-ylmethyl)amino)cyclobut-3-ene-1,2-dione **2t**



Prepared by *Method B* as white solid. Yield: 33.3 mg (8%). ^1H NMR (400 MHz, $\text{DMSO-}d_6$) δ 12.43 (br s, 1H), 9.48 (br s, 1H), 8.63 (d, $J = 4.3$ Hz, 1H), 7.83 (td, $J = 7.7, 1.7$ Hz, 1H), 7.46 (d, $J = 7.8$ Hz, 1H), 7.42 – 7.37 (m, 2H), 7.37 – 7.31 (m, 1H), 7.11 (d, $J = 8.1$ Hz, 1H), 5.01 (d, $J = 5.9$ Hz, 2H), 2.39 (s, 3H). ^{13}C NMR (101 MHz, $\text{DMSO-}d_6$) δ 187.7, 181.6, 170.9, 160.4, 156.7, 155.8, 149.1, 148.2, 137.8, 137.1, 133.0, 125.6, 122.6, 121.4, 116.7, 110.2, 48.0, 21.1. HRMS: m/z : calcd. for $\text{C}_{18}\text{H}_{15}\text{N}_4\text{O}_3^+$: 335.1139 $[\text{M}+\text{H}]^+$; found: 335.1139.

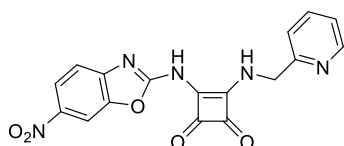
4.2.14.21. 3-((5-Nitrobenzo[d]oxazol-2-yl)amino)-4-((pyridin-2-ylmethyl)amino)cyclobut-3-ene-1,2-dione **2u**



Prepared by *Method B* as white solid. Yield: 71.4 mg (33%). ^1H NMR (400 MHz, $\text{DMSO-}d_6$) δ 9.41 (br s, 1H), 8.57 (d, $J = 4.5$ Hz, 1H), 8.03 (d, $J = 2.1$ Hz, 1H), 7.92 (dd, $J = 8.7, 2.4$ Hz, 1H),

7.81 (td, $J = 7.7, 1.7$ Hz, 1H), 7.49 (d, $J = 8.7$ Hz, 1H), 7.44 (d, $J = 7.8$ Hz, 1H), 7.31 (dd, $J = 7.0, 5.1$ Hz, 1H), 4.97 (d, $J = 6.3$ Hz, 2H). ^{13}C NMR (101 MHz, DMSO- d_6) δ 188.8, 188.3, 175.4, 172.2, 166.5, 158.4, 153.0, 149.0, 144.1, 143.9, 137.0, 122.3, 121.2, 116.9, 109.7, 108.4, 48.1. HRMS: m/z : calcd. for $\text{C}_{17}\text{H}_{12}\text{N}_5\text{O}_5^+$: 366.0833 $[\text{M}+\text{H}]^+$; found: 366.0833.

4.2.14.22. 3-((6-Nitrobenzo[d]oxazol-2-yl)amino)-4-((pyridin-2-ylmethyl)amino)cyclobut-3-ene-1,2-dione **2v**



Prepared by *Method B* as white solid. Yield: 68.7 mg (32%). ^1H NMR (400 MHz, DMSO- d_6) δ 12.99 (br s, 1H), 9.38 (t, $J = 5.9$ Hz, 1H), 8.64 (d, $J = 4.8$ Hz, 1H), 8.49 (d, $J = 2.4$ Hz, 1H), 8.25 (dd, $J = 8.7, 2.4$ Hz, 1H), 7.84 (td, $J = 7.7, 1.9$ Hz, 1H), 7.67 (d, $J = 8.8$ Hz, 1H), 7.48 (d, $J = 7.9$ Hz, 1H), 7.35 (dd, $J = 7.5, 4.9$ Hz, 1H), 5.03 (d, $J = 6.0$ Hz, 2H). ^{13}C NMR (101 MHz, DMSO- d_6) δ 189.0, 188.1, 182.6, 172.2, 160.7, 157.4, 149.6, 148.1, 147.7, 143.0, 137.7, 123.1, 121.9, 117.2, 106.8, 105.4, 48.6. HRMS: m/z : calcd. for $\text{C}_{17}\text{H}_{12}\text{N}_5\text{O}_5^+$: 366.0833 $[\text{M}+\text{H}]^+$; found: 366.0833.

4.3. *In vitro* antimycobacterial activity

4.3.1 Strains and media

The mycobacterial reporter strains used in this study are listed in Table 6. The avirulent *Mycobacterium tuberculosis* (*Mtb*) laboratory strain H37Ra (ATCC[®] 25177[™]), was used as model strain in this study. Despite its limitations such as virulence attenuation and genetic variability compared to clinical isolates, H37Ra remains a useful tool for early-stage drug discovery and development. The cultures were maintained at 37 °C in Middlebrook 7H9 broth (Difco) supplemented with 10% OADC (oleic acid-albumin-dextrose-catalase), 0.05% tyloxapol (Sigma-Aldrich) and 0.4% glycerol or grown on Middlebrook 7H11 agar (Difco) supplemented with 10% OADC and 0.4% glycerol. Hygromycin B (Roche) was added to a final concentration of 100 $\mu\text{g}/\text{ml}$ to the reporter strains mentioned in Table 6.

Table 6: Mycobacterial strains

Strain	Description	Antibiotic resistance
H37Ra	<i>M. tuberculosis</i> H37Ra ATCC [®] 25177 [™]	/

H37Ra-Lux	<i>M. tuberculosis</i> H37Ra Reporter strain: bacterial luciferase hsp60-LuxAB	Hygromycin B (100 µg/ml)
H37Ra.mScarlet ⁺	<i>M. tuberculosis</i> H37Ra Reporter strain: Red fluorescent protein	Hygromycin B (100 µg/ml)

4.3.2. *In vitro* antimycobacterial activity

The antimycobacterial activity was evaluated against H37Ra-Lux. The use of a luminescent strain provides a sensitive, reliable, and quick readout. The test compounds were dissolved in 100% DMSO. It was taken into account that the DMSO concentration remained the same throughout the entire assay and never exceeded 0.5% (v/v). The luminescence of the exponentially growing mycobacterial cultures was measured and adjusted to 5×10^4 RLU/ml, corresponding to approximately 2×10^6 CFU/ml, this standard was used for all following assays.

To obtain the minimal inhibitory concentration (MIC), a dose response assay was performed based on the broth microdilution method as previously described with profound in-house modifications [31,32]. Briefly, a 2-fold nine-point serial dilution was prepared in a stock plate starting from 2 mM. Next, 1 µL was spotted in triplicate in black 96-well plates and H37Ra-Lux was added to a final volume of 200 µL, resulting in a start concentration of 100 µM and 1×10^4 RLU/well. The outer wells were filled with sterile water to prevent evaporation. Each plate contained BDQ as reference drug and a no-growth control and untreated culture serving as positive and negative control, respectively. The plates were incubated at 37 °C for 7 days and readout was performed using the Promega® GloMax Discover plate reader, the plates were shaken orbitally for 1 minute, 50 µL 1% *n*-decanal was injected to each well and luminescence was measured. The data was processed using GraphPad Prism 9, non-linear regression log(inhibitor) vs. response – variable slope (four parameters).

The minimal bactericidal concentration (MBC) was determined based on the setup described above. After 14 days, 2 µL of each test condition was spotted on agar plates in triplicate and full plating was conducted for the wells where MIC was reached and one-step higher concentration. Plates were incubated at 37 °C for 3-4 weeks followed by colony count.

4.3.3. *In vitro* cytotoxicity

Potential drug-induced cytotoxicity was investigated using murine RAW 264.7 (ATCC TIB-71) macrophage cell line. The macrophages were maintained in Dulbecco's Modified Eagle Medium (DMEM) supplemented with 10% iFBS (heat-inactivated fetal bovine serum) at 37 °C in a 5% CO₂ humidified incubator. All test compounds were processed as described above, a

2-fold serial dilution was prepared and 1 μL was spotted in black clear bottom 96 well plates to a final start concentration of 64 μM . 2.5×10^4 cells/ml were seeded to a final volume of 100 μL /well. Tamoxifen served as reference compound, medium and DMSO served as positive and negative control, respectively. Plates were maintained at 37 °C in a 5% CO_2 humidified incubator. 72h post exposure, readout was performed using the standard protocol of CellTiter-Glo® 2.0 (Promega) and data was processed using GraphPad Prism 9, non-linear regression log(inhibitor) vs. response – variable slope (four parameters).

4.3.4. Checkerboard assay

The activity of the most potent squaramides in combination with CFZ was assessed in triplicate in a checkerboard microdilution assay. H37Ra-Lux and antimycobacterial agents were prepared similarly to the antimycobacterial activity assay. A 2-fold serial dilution of each compound was established starting from 2x MIC value. The squaramides were systematically positioned horizontally (column 1-10) and CFZ vertically (row A-G). Luminescent readout was performed after 7 days. Drug combination interactions were reviewed based on the fractional inhibitory concentration indices (FICIs). Which were calculated as follows:

$$\text{FICI} = \text{FIC A} + \text{FIC B} = \frac{\text{A}}{\text{MIC A}} + \frac{\text{B}}{\text{MIC B}}$$

Where A and B are the MIC_{50} s of the antimycobacterial drugs in combination and MIC A and MIC B are the MIC_{50} s of each drug alone. Synergy is defined as $\text{FICI} \leq 0.5$, no interaction or additive effect when the FICI is between 0.5 - 4.0 and antagonism as $\text{FICI} > 4$.

4.3.5. Spontaneous mutant selection.

The methodology was inspired by T. loerger *et al.* [33]. To generate spontaneous mutants, *Mtb* H37Ra was grown under standard conditions to reach exponential phase. Approximately 10^7 bacteria were plated on 7H11 agar plates containing compound concentrations corresponding to 10 and 16 times the predetermined MIC. The plates were incubated at 37 °C for 4-5 weeks until colonies could be observed. Colonies were picked and grown in liquid media supplemented with corresponding compound concentrations.

To validate the resistant clones, gDNA was isolated and primers were designed (Table 7) to amplify and verify all corresponding ATP synthase genes and *rv0678* in which a mutation accounts for a large proportion of BDQ resistant cases, via respectively PCR and Sanger sequencing. The data was analysed using SnapGene (by Dotmatics) software.

After mutant validation, supplementary experiments were performed based on the Resazurin Microtiter Assay (REMA) since luminescence was no longer achievable due to the

lack of a resistant reporter strain. Briefly, 100 μ L of an exponential grown culture diluted to an optical density of 0.02 was dispensed in a black, clear bottomed 96 well plate containing diverse compound concentrations depending on experimental relevance. Subsequent to a 7 day incubation, 20 μ L of 0.02% (w/v) Resazurin was dispensed to each well and incubated for 24h. Next, fluorescence was measured by excitation at 530 nm and emission at 590 nm using the Promega[®] GloMax Discover plate reader.

Table 7: Primer list for mutant screening

Gene	Forward Primer 5'-3'	Reversed Primer 5'-3'
<i>atpA</i>	TCAGCACAAACCGAAGTAGGA	TAGTTCGCGAAGTGTGGCAG
<i>atpB</i>	GGATCGGAAGGAAGGAGCG	TCCTCCTTGATGGCTCTGGT
<i>atpC</i>	GGCCAAGAAAGCCGAGAGT	GCACGACCATGCCGATCAT
<i>atpD</i>	CCAAGCTAGGTTAGCCCCAC	CAATTCGGCCATGCCACAAC
<i>atpE</i>	CGGATGCTGGTAACGGCTA	AGGACAATCGCGCTCACTTC
<i>atpF</i>	CGACGGCAAATGGTTGCAATA	CAGCTGTCCGATAAACGTCG
<i>atpG</i>	GGCGCCGAAGAAGAAGAAAT	GCTTCCTCGTGGGGCTAAC
<i>atpH</i>	TGTTGACCTCACCGCTTCAG	CCTACTTCGGTTTGTGCTGAC
rv0678	GTCTGGTGACGCATACCGAA	ACAAAAACGGTGACCCCA

4.3.6. Macrophage infection

The murine RAW 264.7 (ATCC TIB-71) macrophage cell line was maintained in Dulbecco's Modified Eagle Medium (DMEM) supplemented with 10% iFBS and 1% glutaMAX[™] (Gibco[™]) at 37 °C in a 5% CO₂ humidified incubator. One day prior infection, RAW 264.7 cells were seeded in T75 culture flasks at a density of 5x10⁵ cells/ml (10⁷ cells/flask) in standard medium.

H37Ra-Lux was grown to an exponential phase and harvested in basal uptake buffer (BUB) [34]. The bacterial suspension was transferred through a 25G needle in order to obtain a single-cell suspension of H37Ra-Lux.

Macrophages were infected at a multiplicity of infection (MOI) of 10 in a minimal infection medium consisting of DMEM supplemented with 5% iFBS. After 4h of infection, cells were treated with 200 μ g/ml amikacin for 1h followed by washing the cells with preheated PBS. Subsequently, the infected macrophages were harvested and seeded in black, clear bottom 96-well plates at a density of 2.5x10⁵ cells/ml (5x10⁴ cells/well) in minimal infection media. A 2-fold serial dilution of compounds was prepared in a 100% DMSO stock plate. The concentrations used in the serial dilutions were determined based on the MIC of the respective compounds. Plates were incubated at 37 °C and 5% CO₂ in a humidified incubator. Prior to

the readout, macrophages were washed three times with PBS and lysed using 0.1% triton X-100 (Sigma-Aldrich) for 10 min. 50 μ L of 1% *n*-decanal (Sigma-Aldrich) was injected into each well, and luminescence was measured using a microplate reader (Promega® GloMax Explorer). The readout was performed 24h, 48h and 72h post-infection, and data is displayed as relative light units (RLU).

4.3.7. Immunofluorescence

To monitor intracellular bacteria, RAW 264.7 cells were infected with a red fluorescent reporter strain (H37Ra.mScarlet⁺). Infection was performed as previously described, 5×10^5 infected cells/ml were seeded on sterile coverslips in a 48-well plate. Various concentrations of compound **1d** (8 μ M, 4 μ M and 2 μ M) were added to the macrophages with a final DMSO concentration of 0.5%. Untreated infected cells with 0.5% DMSO medium served as a control. 72h post-infection, cells were washed with PBS and fixed with 4% paraformaldehyde. After washing, actine filaments of macrophages were stained using Fluorescent Dye 488-I Phalloidin (Abnova) (1:1000) for 15 minutes. Subsequently, the nucleus was stained using 1 μ g/ml DAPI for 5 minutes. Finally, the coverslips were washed thoroughly and mounted using a mounting medium (DAKO). The cells were observed and imaged with a ZEISS Axio Observer Z1 microscope at magnitude 63x and ZEN software.

4.4. *In silico* molecular docking

The designed library of ligands was used to generate 3D structures using Marvin 15.1.5, ChemAxon (<http://www.chemaxon.com>). AutoDock Tools program [35] was utilised to add polar hydrogens to all ligands and proteins. Docking of the inhibitor structures from the library into various states of mycobacterial ATP synthase (PDBID:7NJK [state 1a], 7NJP [state 2], 7NJQ [state 3a] [28], 7JGA [state 3 with BDQ] [29] was performed using AutoDock Vina 1.1.2 [27]. The active site of mycobacterial ATP synthase within the crystal structure was the centre of a grid box with an edge length of 21 Å (grid x: 190.5, y: 213.3, z: 138.0). The exhaustiveness parameter was set to 40 (default: 8). Since no experimental structure is available for *Mtb*, we have generated a homology model built using SwissModel server [26] over *Msm* structure PDBID:7NJP.

Declaration of competing interest

The authors declare that they have no known competing financial interests or personal relationships that could have appeared to influence the work reported in this paper.

Acknowledgements

This work was supported by grant no. JG_2019_002 from Palacký University in Olomouc, FWO grant no. G066619N and *via* infrastructure project ELIXIR CZ no. LM2022123 from the Ministry of Education, Youth and Sports of the Czech Republic.

Author contributions

J.C. performed most of the synthetic experiments and analysed the experimental data. L.O. performed most of the biological experiments and analysed the experimental data. M.D. performed the synthesis depicted in Scheme 2. V.Š. synthesised several precursors. V.B. and K.B. carried out molecular docking and homology modelling. L.D.V. supported PhD students with the biological work and reviewed the manuscript. N.S. supported biological assay development and reviewed the manuscript. K.V.C. developed the reporter strains and assisted during the biological experiments. L.V.M. partially performed *in vitro* antimycobacterial activity screening. D.C. was responsible for mycobacterial expertise and screening, planning of the paper, data analysing, funding, and talent acquisition for biology carried out during the research, supervising the PhD students of the biology section. P.C. was responsible for funding acquisition, project administration and supervision of PhD students for the biological work; contributed to the review & editing of the manuscript. L.B. initiated the project, led the project team, was responsible for funding acquisition regarding the synthetic part, designed the synthetic experiments, and analysed the results. L.B. and L.O. co-wrote the paper with input from all authors. All authors have approved the final version of the manuscript.

Appendix A. Supplementary data

Supplementary data to this article can be found online at

References:

- [1] M. Urban, V. Šlachtová, L. Brulíková, Small organic molecules targeting the energy metabolism of *Mycobacterium tuberculosis*, *Eur. J. Med. Chem.* 212 (2021) 113139. <https://doi.org/10.1016/j.ejmech.2020.113139>.
- [2] S. Ahmed, S. Nandi, A.K. Saxena, An updated patent review on drugs for the treatment of tuberculosis (2018-present), *Expert Opin. Ther. Pat.* 32 (2022) 243–260. <https://doi.org/10.1080/13543776.2022.2012151> CO - EOTPEG.
- [3] A. Koul, N. Dendouga, K. Vergauwen, B. Molenberghs, L. Vranckx, R. Willebrords, Z. Ristic, H. Lill, I. Dorange, J. Guillemont, D. Bald, K. Andries, Diarylquinolines target subunit c of mycobacterial ATP synthase, *Nat. Chem. Biol.* 3 (2007) 323–324.
- [4] P. Lu, H. Lill, D. Bald, ATP synthase in mycobacteria: Special features and implications for a function as drug target, *Biochim. Biophys. Acta, Bioenerg.* 1837 (2014) 1208–1218.

- [5] D. Bald, C. Villellas, P. Lu, A. Koul, Targeting energy metabolism in *Mycobacterium tuberculosis*, a new paradigm in antimycobacterial drug discovery, *MBio*. 8 (2017) e00272-17/1-e00272-17/11. <https://doi.org/10.1128/mBio.00272-17>.
- [6] G.M. Courbon, P.R. Palme, L. Mann, A. Richter, P. Imming, J.L. Rubinstein, Mechanism of mycobacterial ATP synthase inhibition by squaramides and second generation diarylquinolines, *EMBO J.* 42 (2023) e113687. <https://doi.org/10.15252/emj.2023113687> CO - EMJODG.
- [7] K. Andries, P. Verhasselt, J. Guillemont, H.W.H. Goehlmann, J.M. Neefs, H. Winkler, J. Van Gestel, P. Timmerman, M. Zhu, E. Lee, P. Williams, D. de Chaffoy, E. Huitric, S. Hoffner, E. Cambau, C. Truffot-Pernot, N. Lounis, V. Jarlier, A Diarylquinoline Drug Active on the ATP Synthase of *Mycobacterium tuberculosis*, *Science* (Washington, DC, United States). 307 (2005) 223–227.
- [8] P.J. Choi, H.S. Sutherland, A.S.T. Tong, A. Blaser, S.G. Franzblau, C.B. Cooper, M.U. Lotlikar, A.M. Upton, J. Guillemont, M. Motte, L. Queguiner, K. Andries, den B.W. Van, W.A. Denny, B.D. Palmer, Synthesis and evaluation of analogues of the tuberculosis drug bedaquiline containing heterocyclic B-ring units, *Bioorg. Med. Chem. Lett.* 27 (2017) 5190–5196.
- [9] C.-J. Qiao, S. Li, C.-J. Qiao, X.-K. Wang, F. Xie, W. Zhong, S. Li, Asymmetric Synthesis and Absolute Configuration Assignment of a New Type of Bedaquiline Analogue, *Molecules* 20 (2015) 22272–22285.
- [10] J.A. Rombouts, R.M.P. Veenboer, C. Villellas, P. Lu, A.W. Ehlers, K. Andries, A. Koul, H. Lill, E. Ruijter, R.V.A. Orru, K. Lammertsma, D. Bald, J.C. Slootweg, Synthesis, characterization and biological activity of fluorescently labeled bedaquiline analogues., *RSC Adv.* 6 (2016) 108708–108716. <https://doi.org/10.1039/C6RA22693K>.
- [11] L. Barbaro, G. Nagalingam, J.A. Triccas, L. Tan, N.P. West, J.B. Baell, D.L. Priebbenow, Synthesis and evaluation of pyridine-derived bedaquiline analogues containing modifications at the A-ring subunit., *RSC Med. Chem.* 12 (2021) 943–959. <https://doi.org/10.1039/d1md00063b>.
- [12] H.S. Sutherland, A.S.T. Tong, P.J. Choi, A. Blaser, S.G. Franzblau, C.B. Cooper, A.M. Upton, M. Lotlikar, W.A. Denny, B.D. Palmer, Variations in the C-unit of bedaquiline provides analogues with improved biology and pharmacology, *Bioorg. Med. Chem.* 28 (2020) 115213.
- [13] A. Blaser, H.S. Sutherland, A.S.T. Tong, P.J. Choi, D. Conole, S.G. Franzblau, C.B. Cooper, A.M. Upton, M. Lotlikar, W.A. Denny, B.D. Palmer, Structure-activity relationships for unit C pyridyl analogues of the tuberculosis drug bedaquiline., *Bioorg. Med. Chem.* 27 (2019) 1283–1291. <https://doi.org/10.1016/j.bmc.2019.02.025>.
- [14] S. Kumar, R. Mehra, S. Sharma, N.P. Bokolia, D. Raina, A. Nargotra, P.P. Singh, I.A.

- Khan, Screening of antitubercular compound library identifies novel ATP synthase inhibitors of *Mycobacterium tuberculosis*, *Tuberculosis* (Oxford, United Kingdom). 108 (2018) 56–63.
- [15] Y.B. Surase, K. Samby, S.R. Amale, R. Sood, K.P. Purnapatre, P.K. Pareek, B. Das, K. Nanda, S. Kumar, A.K. Verma, Identification and synthesis of novel inhibitors of mycobacterium ATP synthase, *Bioorg.Med.Chem.Lett.* 27 (2017) 3454–3459.
- [16] S.J. Tantry, S.D. Markad, V. Shinde, J. Bhat, G. Balakrishnan, A.K. Gupta, A. Ambady, A. Raichurkar, C. Kedari, S. Sharma, N. V Mudugal, A. Narayan, C.N. Naveen Kumar, R. Nanduri, S. Bharath, J. Reddy, V. Panduga, K.R. Prabhakar, K. Kandaswamy, R. Saralaya, P. Kaur, N. Dinesh, S. Guptha, K. Rich, D. Murray, H. Plant, M. Preston, H. Ashton, D. Plant, J. Walsh, P. Alcock, K. Naylor, M. Collier, J. Whiteaker, R.E. McLaughlin, M. Mallya, M. Panda, S. Rudrapatna, V. Ramachandran, R. Shandil, V.K. Sambandamurthy, K. Mdluli, C.B. Cooper, H. Rubin, T. Yano, P. Iyer, S. Narayanan, S. Kavanagh, K. Mukherjee, V. Balasubramanian, V.P. Hosagrahara, S. Solapure, S. Ravishankar, P. Hameed, Discovery of Imidazo[1,2-a]pyridine Ethers and Squaramides as Selective and Potent Inhibitors of Mycobacterial Adenosine Triphosphate (ATP) Synthesis, *J. Med. Chem.* 60 (2017) 1379–1399.
- [17] P. Li, B. Wang, G. Li, L. Fu, D. Zhang, Z. Lin, H. Huang, Y. Lu, Design, synthesis and biological evaluation of diamino substituted cyclobut-3-ene-1,2-dione derivatives for the treatment of drug-resistant tuberculosis., *Eur. J. Med. Chem.* 206 (2020) 112538. <https://doi.org/10.1016/j.ejmech.2020.112538>.
- [18] J. Chasák, V. Šlachťová, M. Urban, L. Brulíková, Squaric acid analogues in medicinal chemistry, *Eur. J. Med. Chem.* 209 (2021) 112872. <https://doi.org/10.1016/j.ejmech.2020.112872>.
- [19] K.A. Agnew-Francis, C.M. Williams, Squaramides as Bioisosteres in Contemporary Drug Design, *Chem. Rev.* (Washington, DC, United States). 120 (2020) 11616–11650. <https://doi.org/10.1021/acs.chemrev.0c00416> CO - CHREAY.
- [20] V.A. Dartois, E.J. Rubin, Anti-tuberculosis treatment strategies and drug development: challenges and priorities, (n.d.). <https://doi.org/10.1038/s41579-022-00731-y>.
- [21] V. Šlachťová, J. Chasák, L. Brulíková, Synthesis of Various 2-Aminobenzoxazoles: The Study of Cyclization and Smiles Rearrangement, *ACS Omega.* 4 (2019) 19314–19323. <https://doi.org/10.1021/acsomega.9b02702>.
- [22] M. Luo, W. Zhou, H. Patel, A.P. Srivastava, J. Symersky, M.M. Bonar, J.D. Faraldo-Gómez, M. Liao, D.M. Mueller, Bedaquiline inhibits the yeast and human mitochondrial ATP synthases, *Commun. Biol.* 2020 31. 3 (2020) 1–10. <https://doi.org/10.1038/s42003-020-01173-z>.
- [23] R.V. Nugraha, V. Yunivita, P. Santoso, R.E. Aarnoutse, R. Ruslami, Clofazimine as a

- Treatment for Multidrug-Resistant Tuberculosis: A Review, *Sci. Pharm.* 2021, Vol. 89, Page 19. 89 (2021) 19. <https://doi.org/10.3390/SCIPHARM89020019>.
- [24] C.A. Lipinski, Lead- and drug-like compounds: The rule-of-five revolution, *Drug Discov. Today Technol.* 1 (2004) 337–341. <https://doi.org/10.1016/j.ddtec.2004.11.007>.
- [25] A. Daina, O. Michielin, V. Zoete, SwissADME: A free web tool to evaluate pharmacokinetics, drug-likeness and medicinal chemistry friendliness of small molecules, *Sci. Rep.* 7 (2017) 1–13. <https://doi.org/10.1038/srep42717>.
- [26] A. Waterhouse, M. Bertoni, S. Bienert, G. Studer, G. Tauriello, R. Gumienny, F.T. Heer, T.A.P. de Beer, C. Rempfer, L. Bordoli, R. Lepore, T. Schwede, SWISS-MODEL: homology modelling of protein structures and complexes, *Nucleic Acids Res.* 46 (2018) W296. <https://doi.org/10.1093/nar/gky427> CO - NARHAD.
- [27] O. Trott, A.J. Olson, AutoDock Vina: Improving the speed and accuracy of docking with a new scoring function, efficient optimization, and multithreading, *J. Comput. Chem.* 31 (2010) 455–461.
- [28] M.G. Montgomery, J. Petri, T.E. Spikes, J.E. Walker, Structure of the ATP synthase from *Mycobacterium smegmatis* provides targets for treating tuberculosis, *Proc. Natl. Acad. Sci. U. S. A.* 118 (2021) e2111899118. <https://doi.org/10.1073/pnas.2111899118> CO - PNASA6.
- [29] H. Guo, G.M. Courbon, S.A. Bueler, J. Mai, J. Liu, J.L. Rubinstein, Structure of mycobacterial ATP synthase bound to the tuberculosis drug bedaquiline, *Nature (London, United Kingdom)*. 589 (2021) 143–147. <https://doi.org/10.1038/s41586-020-3004-3>.
- [30] S. Bhunia, S. Chaudhuri, A. Bisai, Total Syntheses of Pyroclavine, Festuclavine, Lysergol, and Isolysergol via a Catalytic Asymmetric Nitro-Michael Reaction, *Chem. - A Eur. J.* 23 (2017) 11234–11238. <https://doi.org/10.1002/chem.201702459>.
- [31] E. Banfi, G. Scialino, C. Monti-Bragadin, Development of a microdilution method to evaluate *Mycobacterium tuberculosis* drug susceptibility, *J. Antimicrob. Chemother.* 52 (2003) 796–800. <https://doi.org/10.1093/jac/dkg439>.
- [32] T. Schön, J. Werngren, D. Machado, E. Borroni, M. Wijkander, G. Lina, J. Mouton, E. Matuschek, G. Kahlmeter, C. Giske, M. Santin, D.M. Cirillo, M. Viveiros, E. Cambau, Antimicrobial susceptibility testing of *Mycobacterium tuberculosis* complex isolates – the EUCAST broth microdilution reference method for MIC determination, *Clin. Microbiol. Infect.* 26 (2020) 1488–1492. <https://doi.org/10.1016/j.cmi.2020.07.036>.
- [33] T.R. Ioerger, T. O'Malley, R. Liao, K.M. Guinn, M.J. Hickey, N. Mohaideen, K.C. Murphy, H.I.M. Boshoff, V. Mizrahi, E.J. Rubin, C.M. Sassetti, C.E. Barry, D.R. Sherman, T. Parish, J.C. Sacchettini, Identification of New Drug Targets and

- Resistance Mechanisms in *Mycobacterium tuberculosis*, PLoS One. 8 (2013) 1–13.
<https://doi.org/10.1371/journal.pone.0075245>.
- [34] E. V. Nazarova, D.G. Russell, Growing and handling of *Mycobacterium tuberculosis* for macrophage infection assays, Methods Mol. Biol. 1519 (2017) 325.
https://doi.org/10.1007/978-1-4939-6581-6_22.
- [35] G.M. Morris, R. Huey, W. Lindstrom, M.F. Sanner, R.K. Belew, D.S. Goodsell, A.J. Olson, AutoDock and AutoDockTools: Automated docking with selective receptor flexibility, J. Comput. Chem. 30 (2009) 2785–2791.